HHS Public Access

Author manuscript

J Immunol. Author manuscript; available in PMC 2019 March 15.

Published in final edited form as:

J Immunol. 2018 March 15; 200(6): 2140–2153. doi:10.4049/jimmunol.1701442.

Galectin-3 interacts with the CHI3L1 axis and contributes to Hermansky-Pudlak Syndrome Lung Disease

Yang Zhou[1,*], **Chuan Hua He**[1], **Daniel Yang**[1], **Tung Nguyen**[1], **Yueming Cao**[1], **Suchitra Kamle**[1], **Chang-min Lee**[1], **Bernadette R. Gochuico**[2], **William A. Gahl**[2], **Barry S. Shea**[3], **Chun Geun Lee**[1], and **Jack A. Elias**[1,4,*]

[1]Department of Molecular Microbiology and Immunology, Brown University, Providence, R.I. USA

[2]Medical Genetics Branch, National Human Genome Research Institute (NHGRI), NIH, Bethesda, Maryland, USA

[3]Division of Pulmonary, Critical Care and Sleep Medicine, Alpert Medical School of Brown University and Rhode Island Hospital, Providence, Rhode Island, USA

[4]Department of Internal Medicine, Warren Alpert Medical School, Brown University Providence, R.I. USA

Abstract

Hermansky-Pudlak Syndrome (HPS) comprises a group of inherited disorders caused by mutations that alter the function of lysosome-related organelles. Pulmonary fibrosis is the major cause of morbidity and mortality in HPS-1 and HPS-4 patients. However, the mechanisms that underlie the exaggerated injury and fibroproliferative repair responses in HPS have not been adequately defined. In particular, although Galactin-3 (Gal-3) is dysregulated in HPS, its roles in the pathogenesis of HPS have not been adequately defined. In addition, although chitinase 3-like-1 (CHI3L1) and its receptors play major roles in the injury and repair responses in HPS, the ability of Gal-3 to interact with or alter the function of these moieties has not been evaluated. Here we demonstrate that Gal-3 accumulates in exaggerated quantities in bronchoalveolar lavage fluids and trafficks abnormally and accumulates intracellularly in lung fibroblasts and macrophages from bleomycin-treated pale ear, HPS-1 deficient mice. We also demonstrate that Gal-3 drives epithelial apoptosis when in the extracellular space, and stimulates cell proliferation and myofibroblast differentiation when accumulated in fibroblasts and M2-like differentiation when accumulated in macrophages. Biophysical and signaling evaluations also demonstrated that Gal-3 physically interacts with IL-13Rα2 and CHI3L1 and competes with TMEM219 for IL-13Rα2 binding. By doing so, Gal-3 diminishes the antiapoptotic effects of and the antiapoptotic signaling induced by CHI3L1 in epithelial cells while augmenting macrophage Wnt/β-catenin signaling. Thus, Gal-3 contributes to the exaggerated injury and fibroproliferative repair responses in HPS by altering the antiapoptotic and fibroproliferative effects of CHI3L1 and its receptor complex in a tissue compartment-specific manner.

[*]Corresponding author; Jack A. Elias, MD, Senior Vice President for Health Affairs, Dean of Medicine and Biological Sciences, Frank L. Day Professor of Biology, Professor of Medicine, Brown University, Warren Alpert Medical School, 222 Richmond Street, Providence, RI 02903, USA, Yang Zhou, PhD, Assistant Professor of Molecular Microbiology & Immunology, Division of Biology and Medicine, Brown University, Sidney Frank Hall, Room 258, Box G-B5, 185 Meeting Street, Providence, RI 02912, USA.

Introduction

HPS is a group of inherited autosomal recessive disorders that occur worldwide (1–3). Ten genetic subtypes (HPS1–10) have been described with each mutation affecting the function of lysosome-related organelles (LROs) (3, 4). Although pulmonary fibrosis occurs in HPS-2 (5), this fatal complication has been appreciated largely in HPS-1 and HPS-4 patients, whose genetic defects are in biogenesis of lysosome-related organelle complex 3 (BLOC-3), which includes HPS1 and HPS4 proteins (6–11). HPS-1 is particularly common in northwest Puerto Rico where 1:1800 people are affected and the carrier frequency is 1 in 21 persons (12–14). Due to the untreatable and progressive nature of the pulmonary fibrosis of HPS, this complication is the leading cause of death for those with the disorder (15). However, the mechanism(s) by which LRO-related defects lead to the exaggerated injury and fibroproliferative repair responses, defined in HPS and models of the disorder (7, 10, 16–19), have not been adequately defined.

Galectin-3 (Gal-3) is a β-galactoside-binding lectin that is expressed in the nucleus, cytoplasm or within the extracellular milieu of cells from multiple organs including the lung (20, 21). It has pleiotropic effector functions including the ability to regulate cell death responses (22, 23) and tissue fibrosis (20, 21, 24–26). Recent studies from our laboratories demonstrated that the concentrations of Gal-3 in bronchoalveolar lavage (BAL) fluids from HPS patients were significantly higher than in samples from patients with idiopathic pulmonary fibrosis or controls, and correlate with HPS disease severity (27). Additionally, studies demonstrated that dermal fibroblasts from HPS subtypes that are associated with pulmonary fibrosis manifest abnormal Gal-3 trafficking and exaggerated intracellular Gal-3 accumulation compared to cells from controls and HPS subtypes that do not have pulmonary fibrosis (27). However, the roles of Gal-3 in the exaggerated injury and fibroproliferative repair responses in HPS have not been defined. In addition, the possibility that Gal-3 will manifest different effects in different HPS tissue compartments has not been addressed.

Chitinase 3-like 1 (CHI3L1) is a pleiotropic glycoprotein that also inhibits cell death and drives fibroproliferative repair. Its effects are mediated by at least two receptors. One is the multimeric chitosome that includes IL-13α2 and TMEM219 and the other is CRTH2 (28–31). Recent studies from our laboratory demonstrated that the levels of circulating CHI3L1 are higher in HPS patients with pulmonary fibrosis compared to those that remain fibrosis-free, and that these levels correlate with disease severity. Using murine models, we also demonstrated that a defect in CHI3L1 inhibition of epithelial apoptosis and exaggerated CHI3L1-driven fibroproliferation play important roles in HPS fibrosis. We showed that BLOC-3 proteins differentially contribute to the trafficking of CHI3L1 receptor components; IL-13Rα2 trafficked abnormally but CRTH2 trafficked normally in the absence of HPS1. These studies also demonstrated that the abnormal IL-13Rα2 trafficking abrogated the antiapoptotic effects of CHI3L1 and contributed to the enhanced injury responses and sensitivity to apoptosis in BLOC-3 HPS patients and murine models of these disorders (31). In contrast, CHI3L1 drives fibrosis via interactions with CRTH2, which traffics normally in BLOC-3 HPS and HPS-1 deficient mice. When viewed in combination, these studies highlight the importance of the CHI3L1 axis in the exaggerated sensitivity of the epithelium to injury and the augmented fibroproliferative repair response in HPS. They also

demonstrate that IL-13Rα2 and Gal-3 have overlapping effector profiles and that the trafficking of both is dependent on BLOC-3 proteins. However, a relationship between Gal-3 and CHI3L1 and its receptors in HPS has not been defined.

We hypothesized that Gal-3 influences the HPS fibroproliferative repair response in a tissue-specific manner, via interactions with CHI3L1 and or its receptor components. Hence, we characterized the levels of Gal-3 in BAL from bleomycin-treated wild type and HPS-1 deficient mice, characterized the expression and trafficking of Gal-3 in epithelial cells, fibroblasts and macrophages from these animals, and defined the effects of extracellular and intracellular Gal-3 on these cell populations. We also used biophysical approaches to define the interactions of Gal-3, CHI3L1 and components of its receptor complex. These studies demonstrate that Gal-3 is up-regulated in murine models of HPS-associated pulmonary fibrosis and that Gal-3 accumulates intracellularly due to defective trafficking in fibroblasts and macrophages from HPS-1 deficient mice. We also show that extracellular Gal-3 is a potent stimulator of epithelial apoptosis, while intracellular Gal-3 drives fibroproliferative repair by inhibiting fibroblast apoptosis, increasing fibroblast proliferation and myofibroblast transformation, and increasing M2-like macrophage differentiation. Lastly, these studies demonstrated that Gal-3 physically interacts with CHI3L1 and its IL-13Rα2 and TMEM219 receptor components, which abrogates CHI3L1-induced antiapoptotic signaling, augments Wnt/β-catenin signaling, and contributes to the development of epithelial cell death and tissue fibrosis in the lungs of HPS-1 deficient mice.

Materials and Methods

Knockout and transgenic (Tg) mice

Pale ear mice (HPS1$^{-/-}$) and Gal-3 knockout mice were obtained from Jackson Laboratory. *Pale ear*/Gal-3 double mutant mice were generated in our laboratory. All mice were congenic on a C57BL/6 backgroundand were genotyped as previously described (31).

Bleomycin Administration

Sex-matched, 8-wk-old wild-type (WT), *pale ear*, Gal-3$^{-/-}$, and *Pale ear*/Gal-3 double mutant mice mice (≥4 mice/group/experiment, repeated at least 3 times) were exposed to a single bleomycin injection (1.25 U/kg; Teva Parenteral Medicines, Irvine, CA) via intratracheal administration. Mice were sacrificed and evaluated at Day 7 and Day 14 to examine apoptosis and fibrosis, respectively.

mRNA analysis

Total cellular RNA was obtained using TRIzol reagent (Invitrogen), according to the manufacturer's instructions. mRNA was measured using real-time RT-PCR as described previously (32, 33). The primer sequences for extracellular matrix genes were obtained from PrimerBank(*pga.mgh.harvard.edu/primerbank/*) or the same as previously used (32, 34, 35).

ELISA

Gal-3 levels in mouse BAL samples, cell lysates, and cell culture supernantent were quantified using an ELISA kit (R&D Systems) following the manufacturer’s instructions.

Immunofluorescence staining

To localize the expression of Gal-3, double-label immunofluorescence staining was undertaken using Paraffin-embedded lungs from WT and pale ear mice. Monoclonal anti-Gal-3 (Santa Cruz), anti-F4/80 (Abcam), CD68 (Abcam), anti-CHI3L1 (R&D) antibodies were used in these evaluations as previously described (29).

Cell proliferation assay

Cells were seeded (4000 cells per well) in 96 well plates. Water Soluble Tetrazolium Salt-1 (WST1) reagent (Roche, Basel, Switzerland) to detect mitochondrial dehydrogenase enzymes was added directly to cell culture medium between 16 and 24 h after serum starvation. After 1 hour of incubation, the plate was read at 450 nm with equipment reference reading at 630 nm.

Histologic analysis

Mouse lungs were removed en bloc, inflated to 25 cm pressure with PBS containing 0.5% low melting point agarose gel, fixed, embedded in paraffin, sectioned, and stained. Hematoxylin and eosin, and Mallory's trichrome stains were performed in the Research Histology Laboratory at Brown University. BAL and lung inflammation was assessed as described previously (32).

Quantification of lung collagen

Animals were anesthetized, median sternotomy was performed, and right heart perfusion completed with calcium and magnesium-free PBS. The heart and lungs were then removed. The right lung was frozen in liquid nitrogen and stored at −80°C until used. Collagen content was determined by quantifying total soluble collagen using the Sircol Collagen Assay kit (Biocolor, Accurate Chemical & Scientific Co., Westbury, NY) according to the manufacturer's instructions.

TUNEL analysis

End labeling of exposed 3′-OH ends of DNA fragments in paraffin-embedded tissue was undertaken with the TUNEL in situ cell death detection kit AP (Roche Diagnostics). After staining, 8–10 random pictures were obtained from each lung or cell culture well, and a minimum of 200 cells were visually evaluated in each section. The labeled cells were expressed as a percentage of total nuclei.

Cell culture

Primary alveolar macrophages, lung fibroblasts, and Type II lung epithelial cells from WT or *pale ear* mice were used in the experiments. MLE12 cells were obtained from ATCC. Treatments include: recombinant CHI3L1 (500ng/ml), recombinant Gal-3 (100ng/ml), TGF-β (20ng/ml), H_2O_2 (100 μg/ml), Gal-3 siRNA, Gal-3 overexpression construct, and bleomycin (100 μg/ml). Cells were cytospun onto slides for TUNEL analysis as previously described. Cellular RNA or protein were extracted for additional analyses.

Co-immunoprecipitation and Western Blots

Proteins from the lung lysate of WT mice or IL-13 Tg mice were clarified by centrifugation for 10 min at 4 degree. Gal-3, IL-13Rα2, and CHI3L1 were immunoprecipitated with anti-Gal-3 rabbit polyclonal antibody (Santa Cruz sc-53127, against full length Gal-3), anti-CHI3L1 (R&D MAB2649, against the catalytic domain), or anti-IL-13Rα2 monoclonal antibody (R&D AF539, against the extracellular domain), respectively, using Catch and Release V2.0 (Reversible Immunoprecipitation System, EMD Millipore). Similarly, recombinant human proteins were immunoprecipitated with anti-Gal-3 rabbit polyclonal antibody (Santa Cruz sc-53127, against full length Gal-3), anti-CHI3L1 (R&D AF2599, against the catalytic domain), or anti-IL-13Rα2 monoclonal antibody (R&D AF146, against the extracellular domain). The precipitates were subjected to immunoblotting with antibodies against Gal-3, IL-13Rα2, CHI3L1, and TMEM219 (R&D AF7556, against the extracellular domain) respectively. Western blots for signaling were performed as previously described (28, 30).

Equipment & running buffer preparation for SPR

Surface plasmon resonance was conducted at Brown University EPSCOR Proteomics facility with the GE Biacore X100 Plus Package (which includes the in-line buffer degasser that remove air bubbles to minimize their disruption to protein-protein interactions) and analyzed via the Biacore Evaluation Software on the Windows 2000 machine in the facility. HBS-EP+ buffer was diluted 1:10 with MilliQ water (final concentration: 10 mM HEPES, 150 mM NaCl, 3 mM EDTA, and 0.005% Surfactant P20; GE Healthcare Life Sciences BR100826) for use within 24 hours and vacuum steri-filtered using Stericup-GP 250mL Express Plus PES 0.22um (EMD Millipore SCGPU02RE, Darmstadt, Germany) to remove potential debris or precipitates. This buffer was the primary buffer for any interaction studies for the flow system.

Recombinant Proteins for SPR

Proteins involved in these SPR experiments were purchased from ACROBiosystems. Post-translational glycosylation are critical for modulating binding in some situations. Proteins were reconstituted at the manufacturer recommended concentration indicated below in HBS-EP running buffer, the same as the assay running buffer to minimize bulk refraction effect, and frozen in 20 uL aliquots at −80C. Proteins that have been thawed are kept for less than 1 week in 4C.

General protocol of preconcentration optimization & immobilization of ligand onto Sensor Chip CM5

Before immobilizing ligand onto the CM5 chip, the protein Gal-3 required a pre-concentrating pH screen to optimize ionic association of the protein to a non-activated CM5 chip surface, which intrinsically carries a slightly negative charge. Gal-3 was screened for ideal immobilization buffer sodium acetate (10mM NaOAc-HCl or NaOAc-HOAc) buffer pH 4 to pH 5.5 in 0.5 pH increments. When protein was diluted to 40-10 ug/mL concentration in immobilization buffer, which was in most immobilizations a 1:10 dilution, the protein exhibited in theory a positive charge — as the isoelectric point of Gal-3 is above

5.5 — creating ionic interactions with the CM5 chip. The amine coupling strategy via the appropriate Amine Coupling Kit kit (GE Healthcare, BR100050) was employed to covalently link ligand onto the Biacore CM5 Sensor Chip (GE Healthcare, 29149604), a glass slide with a gold cover that is covered with a carboxy-dextran matrix. 0.4 M 1-ethyl-3-(3-dimethylaminopropyl)-carbodiimide (EDC) and 0.1 M N-hydroxysuccinimide (NHS) were each stored when reconstituted with MilliQ-grade water in the −80C and used within 4 months. 1 M ethanolamine-HCl, pH 8.5 was stored, as recommended by Biacore, at 4C and used within 4 months. Upon need to immobilize ligand onto the chip, chip was docked and primed twice with the running buffer. Then, the chip was injected with a 1:1 volume:volume injection of EDC/NHS that had been automatically mixed together seconds ago. This mix was flowed across the chip at 5 ul/s for 7 minutes. Afterwards, ligand (galectin-3 for example) at the specified concentration of either 20 or 10 ug/mL diluted from the 400 ug/mL stock with the appropriate pH NaOAc buffer (in the case of galectin-3, pH 5) was injected into the system in which the HBS-EP running buffer was flowing at 5 ul/s for 7 minutes. Finally, ethanolamine was injected at 5 ul/s for 7 minutes to inactivate active cross-linking residues on the CM5 chip.

SPR binding kinetics studies

Sterifiltered 100 mM alpha-lactose in water was used as regeneration solution with the galectin-3 chip. The regeneration consisted of a 30s injection of the regeneration solution over the galectin-3 coated surface. For kinetic study, samples of analyte (the protein injected into the flow cell to test binding with Gal-3) were serially diluted two-fold from typically 400 nM or 100 nM by the running buffer in the flow system immediately before using the Biacore instrument. Typically, 90–120s analyte injection association was used with between 180–240s dissociation observed for appropriate model fitting. Experiments were done at least three times at various serial dilution patterns in order to establish the kinetic constant values were independent of the concentration of the analyte.

Statistics

Mouse data are expressed as mean ± SEM. As appropriate, groups were compared by ANOVA with Bonferroni's post test; follow-up comparisons between groups were conducted using a two-tailed Student t test. A p value of ≤0.05 was considered to be significant.

Study approval

Animal experiments were approved by the Institutional Animal Care and Use Committee of Brown University in accordance with federal guidelines.

Results

The levels of Galectin-3 are increased in lungs from *pale ear* mice

The *pale ear* mouse has a null mutation of the HPS1 gene and shares many aspects of the human HPS-1 disease phenotype (36, 37). To determine if Gal-3 is dysregulated in *pale ear* mice, the levels of lung lysate Gal-3 mRNA and BAL Gal-3 protein were assessed in wild type (WT) and *pale ear* mice at baseline and after bleomycin challenge. The latter

assessments were undertaken during the fibroproliferative repair phase of the bleomycin response as previously defined (29). At baseline, the levels of Gal-3 mRNA and protein were similar in the lungs of *pale ear* versus WT mice (Fig. 1A,B). In WT mice, bleomycin administration caused a fibroproliferative repair response that was associated with a significant increase in tissue and BAL Gal-3 (Fig. 1A,B). The levels of tissue and BAL Gal-3 in *pale ear* mice exceeded the levels in WT mice after bleomycin treatment (Fig. 1A,B). Immunohistochemical evaluations (IHC) of the lungs from these mice demonstrate that Gal-3 is expressed by inflammatory cells in areas of injury and fibrosis (Fig. 1C). Immunofluorescence staining also demonstrated that macrophages are a major cellular source of Gal-3 in *pale ear* and WT animals (Fig. 1D). These studies demonstrate that the expression and accumulation of Gal-3 are increased during bleomycin-induced fibroproliferative repair in *pale ear* versus control mice.

HPS fibroblasts express and contain more Gal-3 than WT cells and have a Gal-3 trafficking defect

Studies were next undertaken to define the expression and trafficking of Gal-3 in lung fibroblasts from WT and *pale ear* mice. In these experiments we characterized the levels of Gal-3 mRNA and extracellular and intracellular Gal-3 using primary cells from WT and *pale ear* mice before and after stimulation. At baseline, the levels of Gal-3 mRNA in fibroblasts from *pale ear* mice were greater than in cells from WT animals (Fig. 2A). There were also modest increases of intracellular Gal-3 protein levels in cells from *pale ear* mice (Fig. 2B). However, the baseline levels of extracellular Gal-3 were not different in cells from the two groups (Fig. 2C). Treatment with TGF-β1 or H_2O_2 increased the levels of mRNA encoding Gal-3 in fibroblasts from both WT and pale ear mice (Fig. 2A, D). This was associated with increased levels of intracellular Gal-3 in pale ear cells compared to WT controls (Fig. 2B, E). Despite having higher levels of Gal-3 mRNA and higher levels of intracellular Gal-3 than in WT cells, pale ear cells manifested significantly lower levels of Gal-3 secreted into cell culture media after TGF-β1 or H_2O_2 stimulation (Fig. 2C,F). In combination, these findings demonstrate that HPS lung fibroblasts express and contain more Gal-3 than WT cells and have a Gal-3 trafficking defect that augments the intracellular accumulation of Gal-3 and decreases the secretion of Gal-3 into the extracellular space.

HPS macrophages express and contain more Gal-3 than WT cells and have a Gal-3 trafficking defect

To see if the findings noted above were specific for fibroblasts, similar investigations were undertaken using macrophages. As noted in Figure 2G, CHI3L1 treatment increased the levels of Gal-3 mRNA in macrophages from both WT and *pale ear* mice, with the levels in *pale ear* exceeding those in WT cells. In addition, CHI3L1 treatment increased the levels of intracellular Gal-3 accumulation in *pale ear* cells; the levels in HPS cells exceeded those of WT controls (Fig. 2H). In contrast, *pale ear* macrophages manifested significantly lower levels of secreted Gal-3 in cell culture media compared to WT cells (Fig. 2I). Thus, as for the HPS fibroblasts, HPS macrophages expressed and contained more Gal-3 than WT cells and exhibited a Gal-3 trafficking defect that augments the intracellular accumulation of Gal-3 and decreases the secretion of Gal-3 into the extracellular space.

Gal-3 expression and production is not seen in epithelial cells from WT and *pale ear* mice

To determine if Gal-3 was expressed in epithelial cells, alveolar type 2 epithelial cells were isolated from lungs from WT and *pale ear* mice and the levels of Gal-3 mRNA and intracellular and extracellular Gal-3 protein were evaluated before and after stimulation. At baseline Gal-3 mRNA was not readily appreciated in cells from WT or *pale ear* mice (data not shown). In addition, stimulation with TGF-β1, bleomycin or H_2O_2 did not induce levels of intracellular or extracellular Gal-3 that could be appreciated in our evaluations (data not shown). Thus, in contrast to fibroblasts and macrophages, lung epithelial cells did not display induction or production of Gal-3 in WT or *pale ear* mice.

Endogenous Gal-3 regulates apoptosis and fibroproliferative repair *in vivo* in *pale ear* mice

We next compared the bleomycin-induced epithelial injury (apoptosis) and fibroproliferative repair (collagen accumulation) responses in WT mice, Gal-3 null mice, *pale ear* mice, and *pale ear*/Gal-3 double null mutant animals. When compared to the WT controls, bleomycin-challenged pale ear mice manifest exaggerated levels of alveolar Type II cell apoptosis and collagen accumulation (Fig. 3A, B). Importantly, the exaggerated bleomycin-induced epithelial cell death and fibrotic responses in *pale ear* mice were significantly decreased in the absence of Gal-3 (Fig. 3A, B). In accord with the later findings, bleomycin administration increased the levels of mRNA encoding α-smooth muscle actin (α-SMA) in lungs form WT and *pale ear* mice; this inductive response was exaggerated in lungs from *pale ear* animals and this increase was abrogated in *pale ear*/Gal-3 double mutant mice (Fig. 3C). Studies by others have demonstrated that alternatively activated (M2) macrophages play an important role in the development of lung fibrosis (38), either via direct effects on matrix or indirectly by promoting fibroblast accumulation and activation (39, 40). Bleomycin administration increased the levels of mRNA encoding the M2 macrophage marker CD206 in lungs from WT and *pale ear* mice, and this inductive response was exaggerated in lungs from the HPS-1 deficient mice (Fig. 3D). Importantly, the genetic removal of Gal-3 from WT mice or in *pale ear* mice led to significant decreases in pulmonary CD206 expression (Fig. 3D). This was particularly impressive in *pale ear*/Gal-3 double mutant animals whose levels of expression of CD206 after bleomycin treatment were below those in similarly treated WT controls (Fig. 3D). When viewed in combination, these studies demonstrate that bleomycin-treated *pale ear* mice manifest exaggerated levels of epithelial cell apoptosis, pulmonary fibrosis and myofibroblast and M2 macrophage accumulation. They also indicate that Gal-3 plays a key role in these events because the exaggerated apoptosis, fibrosis and myofibroblast and M2 macrophage accumulation in bleomycin-treated *pale ear* mice were eliminated in pale ear/Gal-3 double mutant animals.

Extracellular Gal-3 induces apoptosis of primary lung epithelial cells from *pale ear* mice *in vitro*

Extracellular Gal-3 has been shown to induce, and intracellular Gal-3 to inhibit, cellular apoptosis (22, 23). Because epithelial cell death plays an important role in the pathogenesis of pulmonary fibrosis (41), studies were undertaken to define the effects of Gal-3 on epithelial cell apoptosis. In these experiments, we harvested primary Type II alveolar epithelial cells from *pale ear* mice and WT mice and investigated the effects of extracellular

recombinant Gal-3 (rGal-3), in the presence and absence of bleomycin using TUNEL evaluations. These studies demonstrated that rGal-3 augmented TUNEL staining in epithelial cells from WT mice and *pale ear* mice (Fig. 4A). Moreover, the levels of apoptosis were more pronounced in cells from *pale ear* animals (Fig. 4A). Bleomycin also increased the TUNEL staining of cells from WT and *pale ear* mice (Fig. 4B), and rGal-3 augmented the levels of apoptosis in these bleomycin-treated WT and *pale ear* cells (Figure 4B). Importantly, *pale ear* cells had higher levels of baseline apoptosis, and were more sensitive to rGal-3-induced apoptosis than WT cells (Fig. 4A and 4B). These effects were not mediated by alterations in intracellular Gal-3; the levels of apoptosis were not altered by treatment with Gal-3 siRNA and, as noted above, significant levels of mRNA encoding Gal-3 were not seen in epithelial cells (Supplemental Fig.1A and 1B). In combination, these studies highlight the ability of extracellular Gal-3 to induce epithelial cell apoptosis and the enhanced sensitivity of epithelial cells from *pale ear* mice to the cell death-inducing effects of Gal-3.

Intracellular Gal-3 regulates fibroblast death, proliferation and differentiation *in vitro*

We next investigated the effects of extracellular and intracellular Gal-3 on fibroblast cell death, proliferation, and differentiation. In the first experiments, H_2O_2 was used to induce cellular injury and apoptosis. As can be seen in Figure 5A, H_2O_2 increased the number of TUNEL positive fibroblasts from WT and *pale ear* mice. Importantly, the *pale ear* fibroblasts were relatively resistant to apoptotic stimuli, manifesting ~40% fewer TUNEL+ cells than WT cells (Fig. 5A). Interestingly, this protection appeared to be mediated by intracellular Gal-3 because siRNA-mediated knockdown of Gal-3 increased the levels of H_2O_2-induced apoptosis in *pale ear* cells to levels that were comparable to those in WT cells (Fig. 5A). In addition, overexpression of Gal-3 protected WT and *pale ear* fibroblasts from oxidant-induced cell death (Fig. 5B). Gal-3 mRNA levels were quantitated to confirm the effects of Gal-3 knockdown or overexpression (data not shown). In contrast, extracellular rGal-3 treatment did not have similar effect on fibroblast apoptosis (Supplemental Fig.2A). These results demonstrate that the heightened levels of Gal-3 that are seen in fibroblasts from *pale ear* mice protect them from oxidative stress-mediated cell injury.

To assess the role of Gal-3 on fibroblast proliferation, fibroblasts were incubated with and without TGF-β1. In these experiments TGF-β1 increased the proliferation of fibroblasts from WT and *pale ear* mice (Figure 5C and D). Importantly, the levels of TGF-β1-induced fibroblast proliferation were higher in cells from *pale ear* than cells from WT mice (Fig. 5C and D). These effects were mediated by intracellular Gal-3 because siRNA-mediated knockdown of Gal-3 decreased the levels of TGF-β1-induced proliferation in *pale ear* cells to levels that were comparable to those in WT cells (Fig. 5C). In addition, overexpression of Gal-3 exaggerated the TGF-β1-driven proliferation of *pale ear* cells (Fig. 5D). Gal-3 mRNA levels were quantitated to confirm the effects of Gal-3 knockdown or overexpression (data not shown). In combination, these results demonstrate that the heightened accumulation of Gal-3 in cells from *pale ear* mice augments their proliferative response to TGF-β1.

Studies were also undertaken to define the role(s) of intracellular Gal-3 in myofibroblast differentiation. When the levels of expression of α-SMA were used as a surrogate for

myofibroblast differentiation and accumulation, TGF-β1 was a powerful stimulator of α-SMA in WT and *pale ear* cells; the *pale ear* response exceeded that in the WT cells (Fig. 5E). Gal-3 knockdown reduced the levels of mRNA encoding α-SMA in *pale ear* cells to levels that were comparable to those in WT cells (Fig. 5E). In addition, overexpression of Gal-3 augmented the ability of TGF-β1 to stimulate α-SMA mRNA accumulation in WT and *pale ear* cells (Fig. 5F). In contrast, extracellular rGal-3 treatment did not augment the ability of TGF-β1 to stimulate α-SMA mRNA accumulation (Supplemental Fig.2B). Consistent with the findings with α-SMA expression, Gal-3 knockdown reduced the levels of vimentin expression in *pale ear* and WT cells (Supplemental Fig. 3A), and overexpression of Gal-3 augmented the ability of TGF-β1 to stimulate vimentin expression (Supplemental Fig. 3B). These studies demonstrate that intracellular Gal-3 augments TGF-β1 induced myofibroblast differentiation in WT and HPS1 deficient fibroblasts.

Intracellular Gal-3 regulates macrophage differentiation *in vitro*

Because of the Gal-3 abnormalities that were seen in macrophages we next characterized the effects of Gal-3 on macrophage responses. In the first experiments, macrophages were incubated with H_2O_2 and cell death was assessed using TUNEL assessments. In these experiments extracellular and intracellular Gal-3 did not appear to play a major role in the induction or regulation of macrophage cell death responses because WT and *pale ear* macrophages exhibited similar levels of TUNEL+ cells after H_2O_2 treatment (Fig. 6A) and the siRNA-mediated knockdown or the overexpression of Gal-3 did not reveal differences in the survival of these cell populations (Fig. 6A and 6B). Similarly, exogenous rGal-3 treatment did not have any effect on the survival of these cells (Supplemental Fig. 4A). Thus, Gal-3 does not regulate oxidant induced macrophage apoptosis.

Previous studies from our laboratory and others have highlighted an association between M2 macrophages and pulmonary fibrosis, and have demonstrated that CHI3L1 is a prominent stimulator of M2 macrophage differentiation (29, 32). To address the role(s) of Gal-3 in these responses we characterized the ability of CHI3L1 to induce macrophage CD206 expression (31). In keeping with previous findings from our laboratory, rCHI3L1 was a potent stimulator of CD206 expression by macrophages from WT and *pale ear* mice (Fig. 6C, D). The macrophages from the *pale ear* mice manifested exaggerated M2/CD206 responses when compared to the cells from WT animals (Fig. 6 C). These effects were mediated by intracellular Gal-3 because siRNA-mediated knockdown of Gal-3 decreased the levels of CHI3L1-induced CD206 expression in *pale ear* cells to levels that were comparable to those in WT cells (Fig. 6C). In addition, overexpression of Gal-3 exaggerated the CHI3L1-driven expression of CD206 in WT and pale ear cells (Fig. 6D). Gal-3 mRNA levels were quantitated to confirm the effects of Gal-3 knockdown or overexpression (data not shown). Exogenous rGal-3 treatment did not modulate M2/CD206 responses (Supplemental Fig. 4B). Thus, CHI3L1 promotes M2 macrophage differentiation in a Gal-3-dependent manner.

Gal-3 diminishes the ability of CHI3L1 to activate antiapoptotic signaling pathways

Previous studies from our laboratory demonstrated that CHI3L1 mediates its antiapoptotic effects, at least in part, by activating MAPK kinase and or AKT signaling pathways that

decrease apoptosis (28, 30). Because the present studies demonstrate that Gal-3 is a prominent stimulator of epithelial apoptosis, and previous studies demonstrated that CHI3L1 has profound anti-apoptotic effects, studies were undertaken to determine if Gal-3 could abrogate the antiapoptotic effects and signaling of CHI3L1. In these experiments we treated MLE12 cells with rGal-3 in the presence or absence of rCHI3L1. In accord with our findings using alveolar type 2 cells (described above), rGal-3 was a potent stimulator of apoptosis and CHI3L1 was a potent inhibitor of this response (Fig. 7A). To define the intracellular signaling events associated with these effects, we investigated the effects of rGal-3 on CHI3L1-induced activation of ERK1/2 and AKT using MLE12 cells. In Fig. 7B, ERK and AKT were activated by rCHI3L1, and the activation of ERK and Akt were diminished (Fig. 7B) in cells co-treated with rCHI3L1 and rGal-3. These studies demonstrate that Gal-3 inhibits the antiapoptotic effects of CHI3l1 and CHI3L1-induced antiapoptotic signaling.

Gal-3 plays a critical role in CHIL1-induced Wnt/β-catenin signaling in macrophages

Previous studies from our laboratory demonstrated that CHI3L1 uses IL-13Rα2 to activate Wnt/β-catenin signaling (28). Therefore, we used murine peritoneal macrophages from Gal-3 null mutant mice to evaluate the roles of Gal-3 in this signaling response. These experiments demonstrated that CHI3L1-activated Wnt/β-catenin in murine peritoneal macrophages and that these responses were significantly decreased in the absence of Gal-3 (Fig. 7C). Exogenous rGal-3 treatment did not have a major effect on CHI3L1-activation of Wnt/β-catenin signaling in murine peritoneal macrophages (Supplemental Fig. 4C). Together, these results demonstrate that Gal-3 plays a critical role in CHI3L1-induced Wnt/β-catenin signaling in lung macrophages.

Gal-3 binds to IL-13Rα2 and CHI3L1

Because Gal-3-induced apoptosis was associated with decreased CHI3L1-induced, chitosome-mediated antiapoptotic signaling, studies were undertaken to determine if Gal-3 altered chitosome structure and or function. Because aniapoptotic CHI3L1 signaling requires IL-13Rα2 and TMEM219 (30), studies were first undertaken to determine if Gal-3 bound to either moiety and or altered the aggregation of the IL-13Rα2-TMEM219 receptor complex. Co-immunoprecipitation (Co-IP) evaluations were undertaken with lung lysates from WT and IL-13 Tg mice because IL-13 stimulates IL-13Rα2 and Gal-3 (28, 42). These studies demonstrated that Gal-3 and IL-13Rα2 physically bind to one another because the immunoprecipitation of one always brought down the other (Fig. 8A). Co-IP assays were also used to evaluate the interactions between CHI3L1 and Gal-3. In these experiments, A549 cells were transfected with plasmids containing full-length complementary DNA encoding Myc-tagged Gal-3 or CHI3L1, lysates were generated and Co-IP was undertaken. These studies demonstrated that Gal-3 also physically binds to CHI3L1 (Fig. 8B). Similar results were obtained in Co-IP experiments using lung lysates from WT and IL-13 Tg mice (Fig. 8C). In addition, in Biacore surface plasmon resonance (SPR) evaluations, Gal-3 binds IL-13Rα2 in a 1:1 model with an approximately 1 nM KD value (data not shown). In addition, Gal-3 binds CHI3L1 with moderate affinity (KD=~94 nM) with biphasic curve fitting (data not shown). In accord with these findings, co-localization studies using multiple label IHC demonstrated that Gal-3 and CHI3L1 were similarly expressed in the cytoplasm and to a lesser degree in nuclei of the lung cells (Fig. 8D), many of which were CD68+

macrophages (Fig. 8E). In combination, these studies demonstrate that Gal-3 physically interacts with IL-13Rα2 and CHI3L1.

Gal-3 competes with TMEM219 for IL-13Rα2

Previous studies from our laboratory demonstrated that optimal CHI3L1-induced antiapoptotic signaling requires CHI3L1 interaction with IL-13Rα2 which, in turn, recruits TMEM219 to the multimeric complex (30). Thus, studies were undertaken to determine if Gal-3 altered the binding of IL-13Rα2 and TMEM219. Hence, co-IP experiments were undertaken using recombinant proteins. These studies confirmed our previous findings that Gal-3 binds to CHI3L1 (Fig. 9A) and IL-13Rα2 (Fig. 9B). Importantly, Gal-3 competed with TMEM219 for IL-13Rα2 binding; rhGal-3 diminished the binding between TMEM219 and IL-13Rα2 (Fig. 9C). These findings demonstrate that Gal-3 can abrogate the formation of the IL-13Ra2/TMEM219 chitosome complex and, in so doing, diminish chitosome antiapoptotic signaling.

Discussion

HPS is an autosomal recessive genetic disorder associated with highly penetrant pulmonary fibrosis that develops in the 4^{th} and 5^{th} decades of life and is the leading cause of death in HPS 1 and 4 patients (2–4, 6–10, 31). HPS patients can also experience many other clinical manifestations including occulocutaneous albinism and a bleeding diathesis (13, 43). Studies of HPS patients have implicated the abnormal trafficking of melanosome in the pigment-related dermal and ocular abnormalities and abnormal formation of platelet granules in the bleeding diathesis (13, 43–47). However, in spite of these conceptual advances that highlight the importance of LRO and vesicle trafficking, the pathogenesis of the pulmonary fibrosis in HPS patients is poorly understood. Specifically, the LRO-related mechanisms that underlie the exaggerated injury and fibroproliferative repair responses in HPS have not been defined and therapeutics have not been identified to alter these survival-limiting responses. Previous studies from our laboratories demonstrated that the levels of Gal-3 are increased in the lungs and BAL fluids from patients with HPS, and that Gal-3 traffics abnormally in dermal fibroblasts from HPS patients prone to lung fibrosis (27). However, the contributions that Gal-3 makes to the pathogenesis of HPS have not been defined.

To address these issues, we characterized the roles of Gal-3 in the pulmonary fibrosis responses of HPS-1 deficient *pale ear* mice. These studies demonstrate that the levels of Gal-3 are increased in BAL fluids from *pale ear* mice and that Gal-3 trafficks abnormally and accumulates in exaggerated quantities intracellularly in fibroblasts and macrophages from HPS-1-deficient animals. They also demonstrate that Gal-3 induces epithelial apoptosis when in the extracellular space, inhibits apoptosis in the intracellular space and stimulates fibroblast proliferation, myofibroblast differentiation and accumulation and M2-like macrophage differentiation in fibroblast and macrophages, respectively. Lastly, these studies also demonstrate that Gal-3 physically binds to CHI3L1 and IL-13Rα2 and competes with TMEM219 for binding to IL-13Rα2, which abrogates CHI3L1-induced IL-13Rα2-mediated antiapoptotic signaling and increases Wnt/β-catenin signaling. In combination, these studies demonstrate that the dysregulation of Gal-3 plays a key role in the pathogenesis of HPS,

contributing in a variety of ways to the exaggerated injury response and exaggerated fibroproliferative repair response that characterize this disorder by interacting with CHI3L1 and its receptors in a compartment-specific manner.

Studies from our laboratory and others have demonstrated that injury and apoptosis are prerequisites for the development of fibrosis and tissue remodeling (29, 31, 41). In keeping with this well documented paradigm, epithelial apoptosis and enhanced fibroproliferative repair are well know to co-exist in tissues from patients with diseases like idiopathic pulmonary fibrosis (IPF) and HPS pulmonary fibrosis (19, 36, 37, 48–50). In contrast to fibrotic disorders such as radiation pneumonitis, in which the initiating injury is known, the fibrosis in HPS occurs spontaneously. This is likely the result of the well-documented enhanced sensitivity of cells and tissues from these patients and their murine models to apoptosis-inducing stimuli (31, 37, 48). The present studies contribute to our understanding of the mechanisms that underlie this enhanced sensitivity by highlighting multiple mechanisms that likely contribute to these exaggerated cell death responses. Specifically, they demonstrate that extracellular Gal-3 is a potent inducer of epithelial apoptosis. This is in keeping with prior studies that showed that extracellular Gal-3 induces apoptosis by activating mitochondrial apoptosis pathways (23). Second, they demonstrate that Gal-3 physically binds to the antiapoptotic ligand CHI3L1 and its receptor IL-13Rα2 and blocks TMEM219 binding to IL-13Rα2. The importance of IL-13Rα2 and the binding of TMEM219 to IL-13Rα2 in CHI3L1-induced antiapoptotic effector and signaling responses was previously described by our laboratory (28, 30). These Gal-3 interactions decrease CHI3L1 activation of antiapoptotic signaling pathways such as Erk1/2 and Akt/Protein Kinase B. Prior studies from our laboratory also demonstrated that there is a trafficking defect of IL-13Rα2 in epithelial cells in HPS-1 deficient mice (31). This likely exaggerates the apoptosis-inducing effects of Gal-3 by limiting the amount of IL-13Rα2 that can combine with TMEM219 to form antiapototic signaling chitosome complexes in HPS epithelial cells. Interestingly, the present studies also demonstrate that CHI3L1 is also a potent stimulator of Gal-3. One can speculate that injury induces CHI3L1 which, in turn, increases the levels of extracellular Gal-3 that enhances the sensitivity of HPS epithelial cells to apoptotic stimuli directly and by interacting with CHI3L1 and its receptor components.

Tissue fibrosis is characterized by a decrease in epithelial cells, increased levels of epithelial cell apoptosis and the accumulation of myofibroblasts that show remarkable resistance to apoptotic stimuli (51, 52). Tissue fibrosis is also associated with the accumulation of M2-like macrophages whose contributions to the pathogenesis of tissue fibrosis are well documented (53, 54). The mechanisms by which epithelial cells are induced to undergo apoptosis, while nearby myofibroblasts become apoptosis-resistant, have long puzzled students of pulmonary fibrosis (55, 56). Nor have the mechanisms by which macrophages undergo M2-like differentiation been adequately defined. The present studies advance our understanding of the mechanisms that likely underlie these responses in HPS and possibly other fibrotic disorders. As noted above, they demonstrate that Gal-3 trafficks abnormally and accumulates in fibroblasts and macrophages but is not produced in detectable quantities by epithelial cells in HPS-1 deficient mice. They also show that intracellular Gal-3 is a potent inhibitor of fibroblast apoptosis, while stimulating fibroblast proliferation and

myofibroblast differentiation. This is in keeping with the known sequence similarities between Gal-3 and the apoptosis inhibitor Bcl-2 (22). Furthermore, the current studies demonstrate that Gal-3 is a potent stimulator of M2 macrophage differentiation *in vivo* and *in vitro*. One can easily see how these effects can contribute to the accumulation of myofibroblasts, as well as the M2 macrophages in HPS and the profibrotic effects of Gal-3 that have been reported in the liver (24), kidney (25), lung (20) and in scleroderma (26).

CHI3L1 is a member of the 18 glycosyl hydrolase (18 GH) gene family that binds to but does not degrade chitin polysaccharides. It is present in the circulation of normal individuals and is present in exaggerated quantities in the circulation of patients with a variety of diseases, many of which are characterized by inflammation, injury, repair and or tissue remodeling (32, 33, 57–59). Recent studies from our laboratory and others have demonstrated that CHI3L1 plays critical roles in antipathogen, antigen-induced, and oxidant mediated responses by regulating essential biologic responses including cell death, inflammasome activation, Th1/Th2 cytokine balance, macrophage differentiation and accumulation and Erk, Akt and Wnt/β-catenin signaling (32, 33, 57, 60–63). In many of these settings, CHI3L1 is likely produced as a protective response based on its ability to simultaneously decrease epithelial apoptosis and stimulate fibroproliferative repair (29, 31). To understand the mechanisms by which CHI3L1 mediates these responses CHI3L1 receptors/binding partners have been sought and characterized. These studies defined a multimeric receptor called the chitosome, which contains IL-13Rα2 and its co-receptor TMEM219 (28, 30). They also demonstrated that the ability of CHI3L1 to optimally inhibit epithelial cell death and activate Erk1/2 and Akt signaling requires IL-13Rα2 and TMEM219 with CHI3L1 binding to IL-13Rα2, which then attracts TMEM219 to the receptor complex (30). In contrast, CHI3L1 activates Wnt/β-catenin signaling via a pathway that requires IL-13Rα2 but is independent of TMEM219 (28, 30). The present studies demonstrate that Gal-3 binds to CHI3L1 and IL-13Rα2 and blocks the binding of TMEM219 to IL-13Rα2. They also indicate that these interactions decrease Erk and Akt signaling while augmenting Wnt/β-catenin signaling. At present it is not entirely clear how these physical interactions occur. However, one could speculate that IL-13Rα2 is an alpha receptor subunit that can interact with two β-subunit co-receptors, TMEM219 and Gal-3. In this construct, CHI3L1 stimulated IL-13Rα2 would interact with TMEM219 to mediate antiapoptotic effector responses while IL-13Rα2 interactions with Gal-3 would augment apoptotic responses and Wnt/β-catenin activation.

The present studies of Gal-3, along with prior studies of CHI3L1 and its receptors, have provided important new insights into the pathogenesis of pulmonary fibrosis in HPS. They also provide the basis upon which therapies for HPS associated pulmonary fibrosis can be proposed. Specifically, one can easily see how interventions that decrease the production and or accumulation of Gal-3 can be therapeutically useful in this disorder. One can also envision the development of effective combination therapies because Gal-3-based therapies may very well act in an additive or synergistic manner with interventions that augment membrane expression of IL-13Rα2 or block CRTH2. Additional investigations will be required to assess the utility of each of these approaches.

In summary, the present studies demonstrate that Gal-3 is increased in the extracellular space, traffics abnormally, and accumulates in lung fibroblasts and macrophages in mice that lack HPS-1. These abnormalities contribute to the pathogenesis of HPS pulmonary fibrosis, with the extracellular Gal-3 stimulating epithelial apoptosis and intracellular Gal 3 enhancing fibroblast survival and proliferation and myofibroblast and macrophage differentiation. Finally, these effects are mediated by the ability of Gal-3 to bind to CHI3L1 and IL-13Rα2 and block IL-13Rα2-TMEM219 binding, which decreases antiapoptotic and increases Wnt/β-catenin signaling. Additional investigation of the roles of Gal-3 and its interactions with CHI3L1 and its receptors in HPS and related diseases is warranted.

Supplementary Material

Refer to Web version on PubMed Central for supplementary material.

Acknowledgments

Funding: American Thoracic Society/Hermansky-Pudlak Syndrome Network (YZ); U54 GM115677 (YZ & BSS); P20 GM103652 Pilot (YZ); R01 HL093017, U01 HL108638 (JAE); R01 HL115813 (CGL); the Intramural Research Program, NHGRI, NIH (BRG & WAG)

References

1. Gahl, W., Huizing, M. Hermansky-Pudlak Syndrome (October 2012) in: GeneReviews at GeneTests: Medical Genetics Information Resource. [database online]. (Original 2002; Updated 2004, March 2007, September 2012). 2012. Copyright, University of Washington, Seattle, 1997–2010. Available at http://www.genetests.org
2. Seward SL Jr, Gahl WA. Hermansky-pudlak syndrome: health care throughout life. Pediatrics. 2013; 132:153–160. [PubMed: 23753089]
3. El-Chemaly S, Young LR. Hermansky-Pudlak Syndrome. Clinics in chest medicine. 2016; 37:505–511. [PubMed: 27514596]
4. Vicary GW, Vergne Y, Santiago-Cornier A, Young LR, Roman J. Pulmonary Fibrosis in Hermansky-Pudlak Syndrome. Annals of the American Thoracic Society. 2016; 13:1839–1846. [PubMed: 27529121]
5. Gochuico BR, Huizing M, Golas GA, Scher CD, Tsokos M, Denver SD, Frei-Jones MJ, Gahl WA. Interstitial lung disease and pulmonary fibrosis in Hermansky-Pudlak syndrome type 2, an adaptor protein-3 complex disease. Molecular medicine. 2012; 18:56–64. [PubMed: 22009278]
6. Anderson PD, Huizing M, Claassen DA, White J, Gahl WA. Hermansky-Pudlak syndrome type 4 (HPS-4): clinical and molecular characteristics. Hum Genet. 2003; 113:10–17. [PubMed: 12664304]
7. Li W, Rusiniak ME, Chintala S, Gautam R, Novak EK, Swank RT. Murine Hermansky-Pudlak syndrome genes: regulators of lysosome-related organelles. Bioessays. 2004; 26:616–628. [PubMed: 15170859]
8. Brantly M, Avila NA, Shotelersuk V, Lucero C, Huizing M, Gahl WA. Pulmonary function and high-resolution CT findings in patients with an inherited form of pulmonary fibrosis, Hermansky-Pudlak syndrome, due to mutations in HPS-1. Chest. 2000; 117:129–136. [PubMed: 10631210]
9. Chiang PW, Oiso N, Gautam R, Suzuki T, Swank RT, Spritz RA. The Hermansky-Pudlak syndrome 1 (HPS1) and HPS4 proteins are components of two complexes, BLOC-3 and BLOC-4, involved in the biogenesis of lysosome-related organelles. J Biol Chem. 2003; 278:20332–20337. [PubMed: 12663659]
10. Carmona-Rivera C, Simeonov DR, Cardillo ND, Gahl WA, Cadilla CL. A divalent interaction between HPS1 and HPS4 is required for the formation of the biogenesis of lysosome-related

organelle complex-3 (BLOC-3). Biochimica et biophysica acta. 2013; 1833:468–478. [PubMed: 23103514]

11. Hermos CR, Huizing M, Kaiser-Kupfer MI, Gahl WA. Hermansky-Pudlak syndrome type 1: gene organization, novel mutations, and clinical-molecular review of non-Puerto Rican cases. Hum Mutat. 2002; 20:482. [PubMed: 12442288]
12. Avila NA, Brantly M, Premkumar A, Huizing M, Dwyer A, Gahl WA. Hermansky-Pudlak syndrome: radiography and CT of the chest compared with pulmonary function tests and genetic studies. AJR Am J Roentgenol. 2002; 179:887–892. [PubMed: 12239031]
13. Gahl WA, Brantly M, Kaiser-Kupfer MI, Iwata F, Hazelwood S, Shotelersuk V, Duffy LF, Kuehl EM, Troendle J, Bernardini I. Genetic defects and clinical characteristics of patients with a form of oculocutaneous albinism (Hermansky-Pudlak syndrome). The New England journal of medicine. 1998; 338:1258–1264. [PubMed: 9562579]
14. Gahl WA, Brantly M, Troendle J, Avila NA, Padua A, Montalvo C, Cardona H, Calis KA, Gochuico B. Effect of pirfenidone on the pulmonary fibrosis of Hermansky-Pudlak syndrome. Molecular genetics and metabolism. 2002; 76:234–242. [PubMed: 12126938]
15. Pierson DM, Ionescu D, Qing G, Yonan AM, Parkinson K, Colby TC, Leslie K. Pulmonary fibrosis in hermansky-pudlak syndrome. a case report and review. Respiration. 2006; 73:382–395. [PubMed: 16490934]
16. Feng L, Rigatti BW, Novak EK, Gorin MB, Swank RT. Genomic structure of the mouse Ap3b1 gene in normal and pearl mice. Genomics. 2000; 69:370–379. [PubMed: 11056055]
17. Gerondopoulos A, Langemeyer L, Liang JR, Linford A, Barr FA. BLOC-3 mutated in Hermansky-Pudlak syndrome is a Rab32/38 guanine nucleotide exchange factor. Curr Biol. 2012; 22:2135–2139. [PubMed: 23084991]
18. Martina JA, Moriyama K, Bonifacino JS. BLOC-3, a protein complex containing the Hermansky-Pudlak syndrome gene products HPS1 and HPS4. J Biol Chem. 2003; 278:29376–29384. [PubMed: 12756248]
19. Young LR, Gulleman PM, Short CW, Tanjore H, Sherrill T, Qi A, McBride AP, Zaynagetdinov R, Benjamin JT, Lawson WE, Novitskiy SV, Blackwell TS. Epithelial-macrophage interactions determine pulmonary fibrosis susceptibility in Hermansky-Pudlak syndrome. JCI insight. 2016; 1:e88947. [PubMed: 27777976]
20. Mackinnon AC, Gibbons MA, Farnworth SL, Leffler H, Nilsson UJ, Delaine T, Simpson AJ, Forbes SJ, Hirani N, Gauldie J, Sethi T. Regulation of transforming growth factor-beta1-driven lung fibrosis by galectin-3. American journal of respiratory and critical care medicine. 2012; 185:537–546. [PubMed: 22095546]
21. Li LC, Li J, Gao J. Functions of galectin-3 and its role in fibrotic diseases. The Journal of pharmacology and experimental therapeutics. 2014; 351:336–343. [PubMed: 25194021]
22. Yang RY, Hsu DK, Liu FT. Expression of galectin-3 modulates T-cell growth and apoptosis. Proceedings of the National Academy of Sciences of the United States of America. 1996; 93:6737–6742. [PubMed: 8692888]
23. Stillman BN, Hsu DK, Pang M, Brewer CF, Johnson P, Liu FT, Baum LG. Galectin-3 and galectin-1 bind distinct cell surface glycoprotein receptors to induce T cell death. Journal of immunology. 2006; 176:778–789.
24. Henderson NC, Mackinnon AC, Farnworth SL, Poirier F, Russo FP, Iredale JP, Haslett C, Simpson KJ, Sethi T. Galectin-3 regulates myofibroblast activation and hepatic fibrosis. Proceedings of the National Academy of Sciences of the United States of America. 2006; 103:5060–5065. [PubMed: 16549783]
25. Henderson NC, Mackinnon AC, Farnworth SL, Kipari T, Haslett C, Iredale JP, Liu FT, Hughes J, Sethi T. Galectin-3 expression and secretion links macrophages to the promotion of renal fibrosis. The American journal of pathology. 2008; 172:288–298. [PubMed: 18202187]
26. Taniguchi T, Asano Y, Akamata K, Noda S, Masui Y, Yamada D, Takahashi T, Ichimura Y, Toyama T, Tamaki Z, Tada Y, Sugaya M, Kadono T, Sato S. Serum levels of galectin-3: possible association with fibrosis, aberrant angiogenesis, and immune activation in patients with systemic sclerosis. The Journal of rheumatology. 2012; 39:539–544. [PubMed: 22247367]

27. Cullinane AR, Yeager C, Dorward H, Carmona-Rivera C, Wu HP, Moss J, O'Brien KJ, Nathan SD, Meyer KC, Rosas IO, Helip-Wooley A, Huizing M, Gahl WA, Gochuico BR. Dysregulation of galectin-3. Implications for Hermansky-Pudlak syndrome pulmonary fibrosis. American journal of respiratory cell and molecular biology. 2014; 50:605–613. [PubMed: 24134621]
28. He CH, Lee CG, Dela Cruz CS, Lee CM, Zhou Y, Ahangari F, Ma B, Herzog EL, Rosenberg SA, Li Y, Nour AM, Parikh CR, Schmidt I, Modis Y, Cantley L, Elias JA. Chitinase 3-like 1 Regulates Cellular and Tissue Responses via IL-13 Receptor alpha2. Cell Rep. 2013; 4:830–841. [PubMed: 23972995]
29. Zhou Y, Peng H, Sun H, Peng X, Tang C, Gan Y, Chen X, Mathur A, Hu B, Slade MD, Montgomery RR, Shaw AC, Homer RJ, White ES, Lee CM, Moore MW, Gulati M, Geun Lee C, Elias JA, Herzog EL. Chitinase 3-like 1 suppresses injury and promotes fibroproliferative responses in Mammalian lung fibrosis. Sci Transl Med. 2014; 6:240ra276.
30. Lee CM, He CH, Nour AM, Zhou Y, Ma B, Park JW, Kim KH, Dela Cruz C, Sharma L, Nasr ML, Modis Y, Lee CG, Elias JA. IL-13Ralpha2 uses TMEM219 in chitinase 3-like-1-induced signalling and effector responses. Nature communications. 2016; 7:12752.
31. Zhou Y, He CH, Herzog EL, Peng X, Lee CM, Nguyen TH, Gulati M, Gochuico BR, Gahl WA, Slade ML, Lee CG, Elias JA. Chitinase 3-like-1 and its receptors in Hermansky-Pudlak syndrome-associated lung disease. The Journal of clinical investigation. 2015; 125:3178–3192. [PubMed: 26121745]
32. Lee CG, Hartl D, Lee GR, Koller B, Matsuura H, Da Silva CA, Sohn MH, Cohn L, Homer RJ, Kozhich AA, Humbles A, Kearley J, Coyle A, Chupp G, Reed J, Flavell RA, Elias JA. Role of breast regression protein 39 (BRP-39)/chitinase 3-like-1 in Th2 and IL-13-induced tissue responses and apoptosis. The Journal of experimental medicine. 2009; 206:1149–1166. [PubMed: 19414556]
33. Sohn MH, Kang MJ, Matsuura H, Bhandari V, Chen NY, Lee CG, Elias JA. The chitinase-like proteins breast regression protein-39 and YKL-40 regulate hyperoxia-induced acute lung injury. American journal of respiratory and critical care medicine. 2010; 182:918–928. [PubMed: 20558631]
34. Zhou Y, Lee JY, Lee CM, Cho WK, Kang MJ, Koff JL, Yoon PO, Chae J, Park HO, Elias JA, Lee CG. Amphiregulin, an Epidermal Growth Factor Receptor Ligand, Plays an Essential Role in the Pathogenesis of Transforming Growth Factor-beta-induced Pulmonary Fibrosis. The Journal of biological chemistry. 2012; 287:41991–42000. [PubMed: 23086930]
35. Kang HR, Lee CG, Homer RJ, Elias JA. Semaphorin 7A plays a critical role in TGF-beta1-induced pulmonary fibrosis. The Journal of experimental medicine. 2007; 204:1083–1093. [PubMed: 17485510]
36. Young LR, Borchers MT, Allen HL, Gibbons RS, McCormack FX. Lung-restricted macrophage activation in the pearl mouse model of Hermansky-Pudlak syndrome. Journal of immunology. 2006; 176:4361–4368.
37. Young LR, Pasula R, Gulleman PM, Deutsch GH, McCormack FX. Susceptibility of Hermansky-Pudlak mice to bleomycin-induced type II cell apoptosis and fibrosis. American journal of respiratory cell and molecular biology. 2007; 37:67–74. [PubMed: 17363777]
38. Pechkovsky DV, Prasse A, Kollert F, Engel KM, Dentler J, Luttmann W, Friedrich K, Muller-Quernheim J, Zissel G. Alternatively activated alveolar macrophages in pulmonary fibrosis-mediator production and intracellular signal transduction. Clin Immunol. 2010; 137:89–101. [PubMed: 20674506]
39. Gordon S. Alternative activation of macrophages. Nature reviews. Immunology. 2003; 3:23–35.
40. Martinez FO, Gordon S, Locati M, Mantovani A. Transcriptional profiling of the human monocyte-to-macrophage differentiation and polarization: new molecules and patterns of gene expression. Journal of immunology. 2006; 177:7303–7311.
41. Lee CG, Cho SJ, Kang MJ, Chapoval SP, Lee PJ, Noble PW, Yehualaeshet T, Lu B, Flavell RA, Milbrandt J, Homer RJ, Elias JA. Early growth response gene 1-mediated apoptosis is essential for transforming growth factor beta1-induced pulmonary fibrosis. The Journal of experimental medicine. 2004; 200:377–389. [PubMed: 15289506]

42. MacKinnon AC, Farnworth SL, Hodkinson PS, Henderson NC, Atkinson KM, Leffler H, Nilsson UJ, Haslett C, Forbes SJ, Sethi T. Regulation of alternative macrophage activation by galectin-3. Journal of immunology. 2008; 180:2650–2658.
43. Hermansky F, Pudlak P. Albinism associated with hemorrhagic diathesis and unusual pigmented reticular cells in the bone marrow: report of two cases with histochemical studies. Blood. 1959; 14:162–169. [PubMed: 13618373]
44. Tsilou ET, Rubin BI, Reed GF, McCain L, Huizing M, White J, Kaiser-Kupfer MI, Gahl W. Milder ocular findings in Hermansky-Pudlak syndrome type 3 compared with Hermansky-Pudlak syndrome type 1. Ophthalmology. 2004; 111:1599–1603. [PubMed: 15288994]
45. Parker MS, Rosado Shipley W, de Christenson ML, Slutzker AD, Carroll FE, Worrell JA, White JG. The Hermansky-Pudlak syndrome. Ann Diagn Pathol. 1997; 1:99–103. [PubMed: 9869831]
46. Schinella RA, Greco MA, Cobert BL, Denmark LW, Cox RP. Hermansky-Pudlak syndrome with granulomatous colitis. Ann Intern Med. 1980; 92:20–23. [PubMed: 7350869]
47. Mahadeo R, Markowitz J, Fisher S, Daum F. Hermansky-Pudlak syndrome with granulomatous colitis in children. J Pediatr. 1991; 118:904–906. [PubMed: 1674961]
48. Young LR, Gulleman PM, Bridges JP, Weaver TE, Deutsch GH, Blackwell TS, McCormack FX. The alveolar epithelium determines susceptibility to lung fibrosis in Hermansky-Pudlak syndrome. American journal of respiratory and critical care medicine. 2012; 186:1014–1024. [PubMed: 23043085]
49. Selman M, Pardo A. Role of epithelial cells in idiopathic pulmonary fibrosis: from innocent targets to serial killers. Proceedings of the American Thoracic Society. 2006; 3:364–372. [PubMed: 16738202]
50. Zoz DF, Lawson WE, Blackwell TS. Idiopathic pulmonary fibrosis: a disorder of epithelial cell dysfunction. The American journal of the medical sciences. 2011; 341:435–438. [PubMed: 21613930]
51. Thannickal VJ, Horowitz JC. Evolving concepts of apoptosis in idiopathic pulmonary fibrosis. Proceedings of the American Thoracic Society. 2006; 3:350–356. [PubMed: 16738200]
52. Kulasekaran P, Scavone CA, Rogers DS, Arenberg DA, Thannickal VJ, Horowitz JC. Endothelin-1 and transforming growth factor-beta1 independently induce fibroblast resistance to apoptosis via AKT activation. American journal of respiratory cell and molecular biology. 2009; 41:484–493. [PubMed: 19188658]
53. Wynn TA, Vannella KM. Macrophages in Tissue Repair, Regeneration, and Fibrosis. Immunity. 2016; 44:450–462. [PubMed: 26982353]
54. Byrne AJ, Maher TM, Lloyd CM. Pulmonary Macrophages: A New Therapeutic Pathway in Fibrosing Lung Disease? Trends in molecular medicine. 2016; 22:303–316. [PubMed: 26979628]
55. Selman M, Pardo A. Idiopathic pulmonary fibrosis: an epithelial/fibroblastic cross-talk disorder. Respiratory research. 2002; 3:3. [PubMed: 11806838]
56. Sakai N, Tager AM. Fibrosis of two: Epithelial cell-fibroblast interactions in pulmonary fibrosis. Biochimica et biophysica acta. 2013; 1832:911–921. [PubMed: 23499992]
57. Dela Cruz CS, Liu W, He CH, Jacoby A, Gornitzky A, Ma B, Flavell R, Lee CG, Elias JA. Chitinase 3-like-1 promotes Streptococcus pneumoniae killing and augments host tolerance to lung antibacterial responses. Cell Host Microbe. 2012; 12:34–46. [PubMed: 22817986]
58. Lee CG, Da Silva CA, Dela Cruz CS, Ahangari F, Ma B, Kang MJ, He CH, Takyar S, Elias JA. Role of chitin and chitinase/chitinase-like proteins in inflammation, tissue remodeling, and injury. Annu Rev Physiol. 2011; 73:479–501. [PubMed: 21054166]
59. Lee CG, Elias JA. Role of breast regression protein-39/YKL-40 in asthma and allergic responses. Allergy Asthma Immunol Res. 2010; 2:20–27. [PubMed: 20224674]
60. Areshkov PO, Avdieiev SS, Balynska OV, Leroith D, Kavsan VM. Two closely related human members of chitinase-like family, CHI3L1 and CHI3L2, activate ERK1/2 in 293 and U373 cells but have the different influence on cell proliferation. Int J Biol Sci. 2012; 8:39–48. [PubMed: 22211103]
61. Chen C-C, Llado V, Eurich K, Tran HT, Mizoguchi E. Carbohydrate-binding motif in chitinase 3-like 1 (CH13L1/YKL-40) specifically activates Akt signaling pathway in colonic epithelial cells. Clin. Immunol. 2011; 140:268–275. [PubMed: 21546314]

62. Kim MN, Lee KE, Hong JY, Heo WI, Kim KW, Kim KE, Sohn MH. Involvement of the MAPK and PI3K pathways in chitinase 3-like 1-regulated hyperoxia-induced airway epithelial cell death. Biochem Biophys Res Commun. 2012; 421:790–796. [PubMed: 22554524]

63. Matsuura H, Hartl D, Kang MJ, Dela Cruz CS, Koller B, Chupp GL, Homer RJ, Zhou Y, Cho WK, Elias JA, Lee CG. Role of Breast Regression Protein (BRP)-39 in the Pathogenesis of Cigarette Smoke-Induced Inflammation and Emphysema. American journal of respiratory cell and molecular biology. 2011; 44(6):777–86. [PubMed: 20656949]

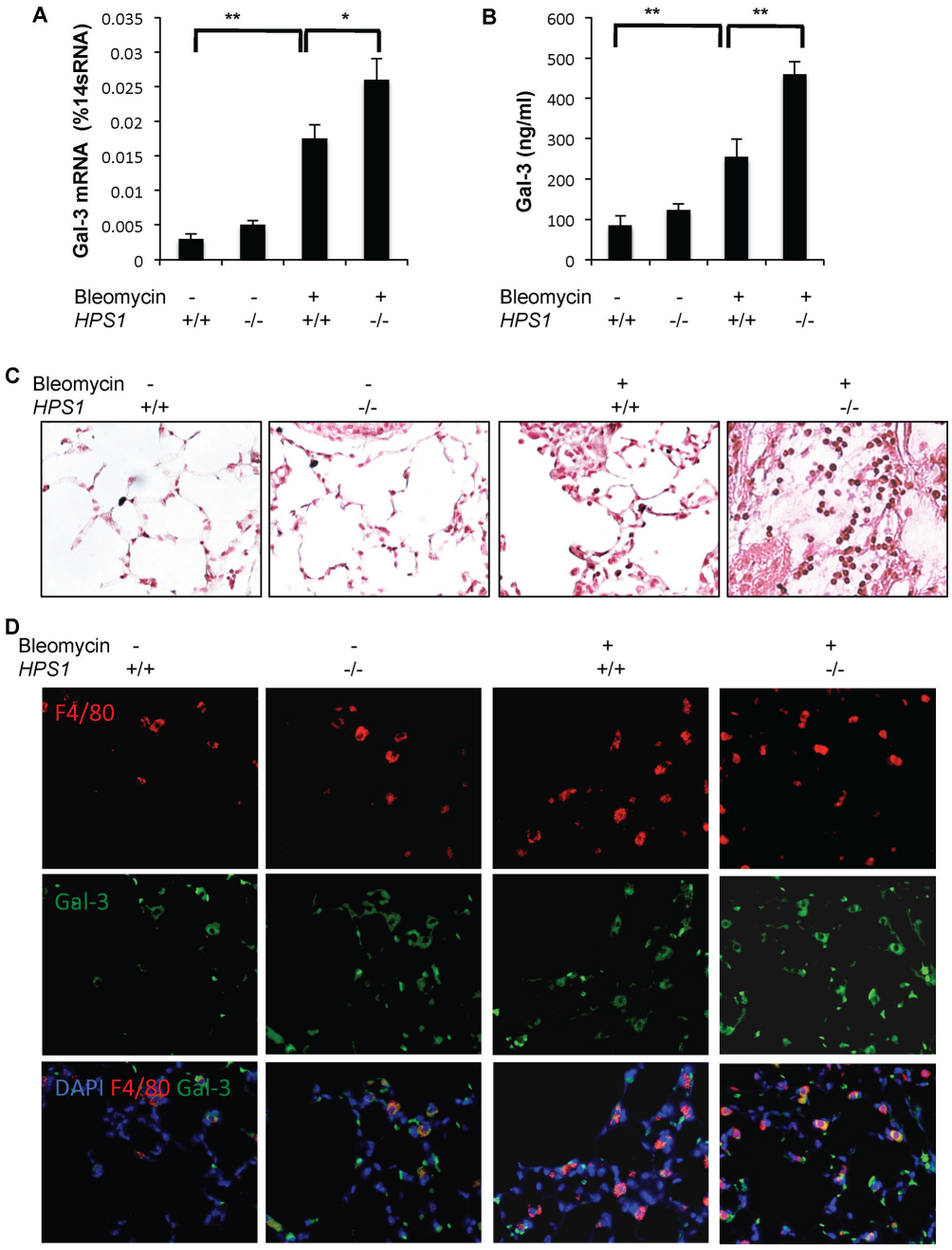

Figure 1. Gal-3 levels are increased in the lungs of *pale ear* mice

WT and *pale ear* mice (*HPS1*$^{-/-}$) were subjected to intratracheal PBS or bleomycin administration and evaluated 14 days later. (A) The levels of whole lung mRNA encoding Gal-3 were assessed using qRT-PCR. (B) The levels of BAL Gal-3 protein were quantified using ELISA evaluations. Values are mean ± SEM with a minimum of 4 mice in each group. Each experiment was undertaken at least 3 times. **p ≤ 0.01,*p ≤ 0.05. (C) Lungs were harvested and lung sections were stained for Gal-3. (D) Lung sections were stained for Gal-3 (green), and co-stained for F4/80 (red). Co-localization is indicated by yellow. Images are representative of 3 mice.

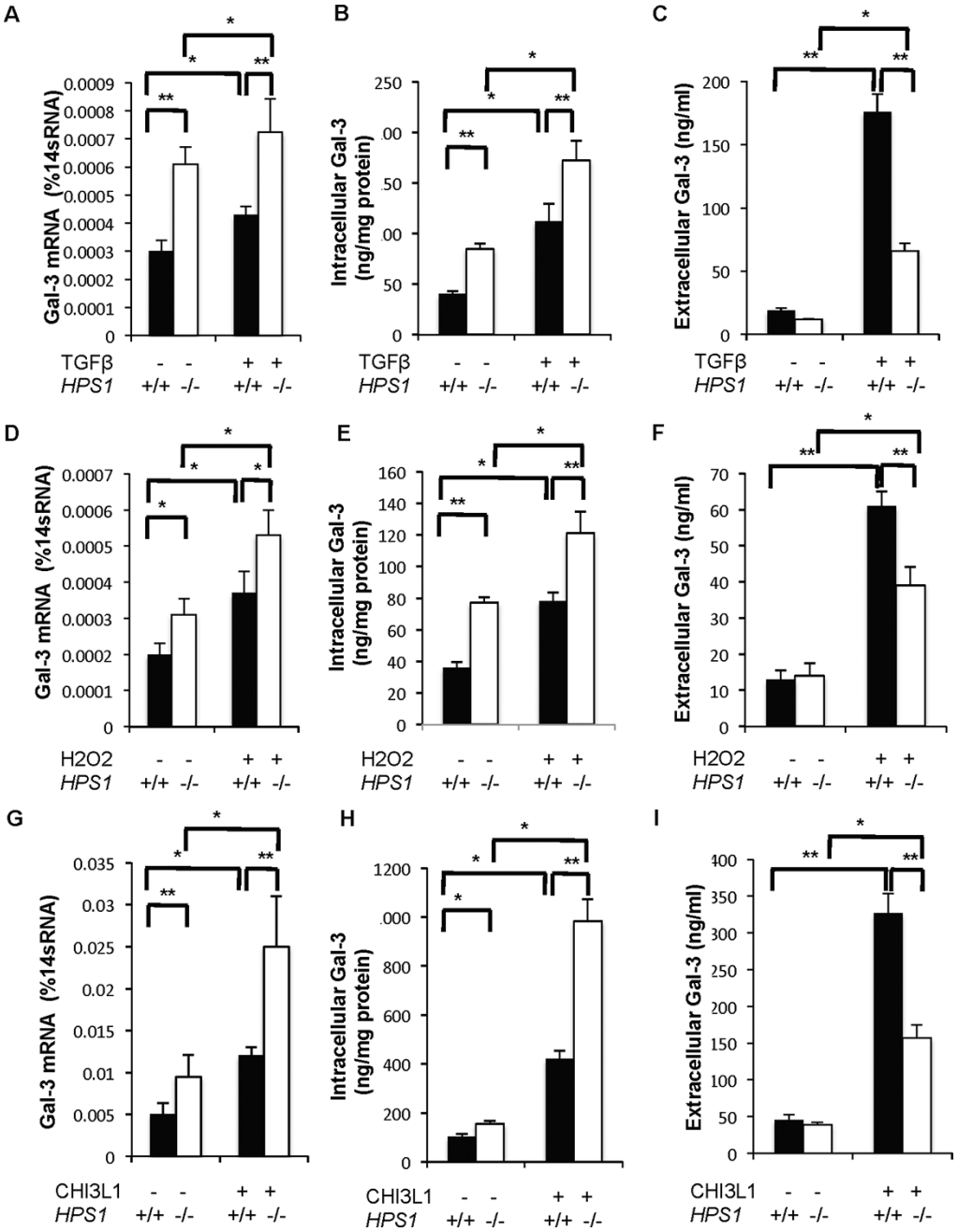

Figure 2. HPS fibroblasts and macrophages make more Gal-3 than WT cells, and have Gal-3 trafficking defects

Primary lung fibroblasts were isolated from WT and *pale ear* mice ($HPS1^{-/-}$) and treated with TGF-β1 or H_2O_2. (A) The levels of mRNA encoding Gal-3 in fibroblasts were assessed using qRT-PCR. (B) Fibroblast lysates were prepared and the levels of intracellular Gal-3 protein were quantified using ELISA evaluations. (C) Fibroblast cell culture supernatants were harvest and the levels of extracellular Gal-3 protein were quantified using ELISA evaluations. (D) The levels of fibroblast mRNA encoding Gal-3 were assessed using qRT-PCR. (E) Fibroblast lysates were prepared and the levels of intracellular Gal-3 protein were quantified using ELISA. (F) Fibroblast cell culture supernatants were harvest and the levels

of extracellular Gal-3 protein were quantified using ELISA evaluations. In panels G-I, primary alveolar macrophages were isolated from WT and *pale ear* mice (*HPS1*$^{-/-}$) and treated with CHI3L1 or vehicle control. (G) The levels of mRNA encoding Gal-3 were measured in RNA extracts using qRT-PCR. (H) Cell lysates were prepared and the levels of intracellular Gal-3 protein were quantified using ELISA evaluations. (I) Macrophage cell culture supernatant were harvested and extracellular Gal-3 protein levels were quantified using ELISA evaluations. Each experiment was undertaken at least 3 times. Values are the mean ± SEM of a minimum of 3 evaluations. **$p \leq 0.01$,*$p \leq 0.05$.

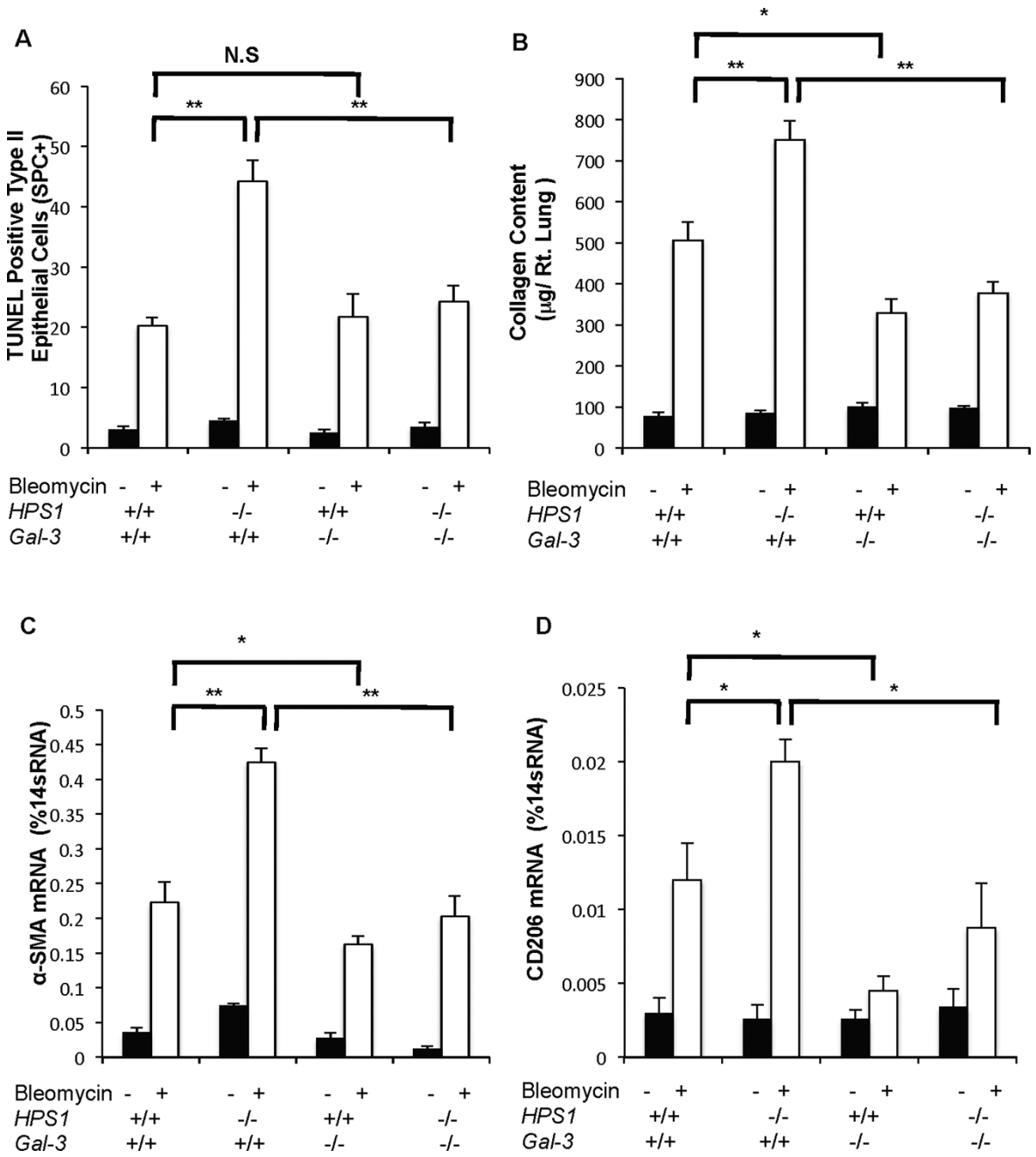

Figure 3. Gal-3 regulates apoptosis and fibroproliferative repair in *pale ear* mice *in vivo*

WT, *pale ear* mice ($HPS1^{-/-}$), Gal-3 null mice ($Gal\text{-}3^{-/-}$), and $HPS1^{-/-}$Gal-$3^{-/-}$ mice were subjected to intratracheal PBS or bleomycin administration. (A) TUNEL staining was performed on Day 7 and TUNEL-positive Type II epithelial cells were counted. (B) Total lung collagen was quantified using Sircol assays on Day 14. (C and D) Total lung mRNA was extracted and α-SMA and CD206 expression levels were determined by RT-PCR. The noted values represent the mean ± SEM of evaluations on a minimum of 4 mice. Each experiment was undertaken at least 3 times. $^{**}p \leq 0.01$,$^{*}p \leq 0.05$.

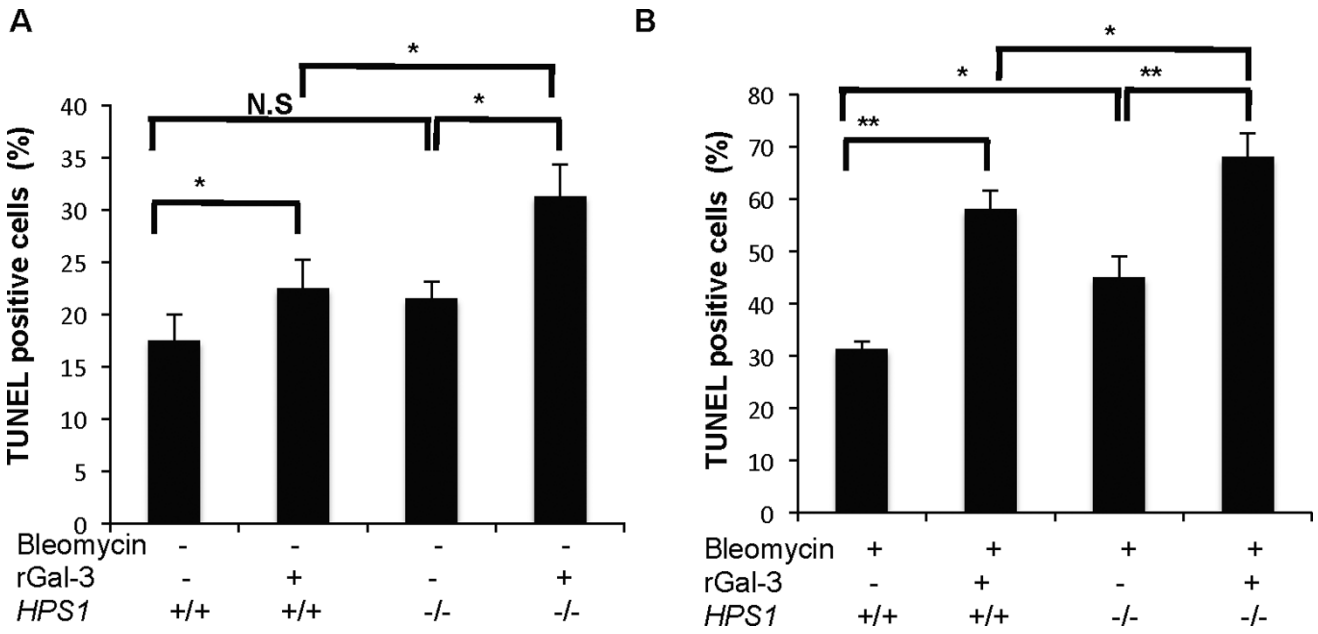

Figure 4. Effects of extracellular Gal-3 on the survival of epithelial cells from WT and *pale ear* mice

Primary Type II alveolar epithelial cells were harvested from WT and *pale ear* mice, pre-treated with recombinant Gal-3 and treated with (A) PBS or (B) bleomycin *in vitro*. TUNEL staining was performed and TUNEL-positive cells were counted. Each experiment was undertaken at least 3 times. The noted values represent the mean ± SEM of 3 separate evaluations. *$p \leq 0.05$,**$p \leq 0.01$.

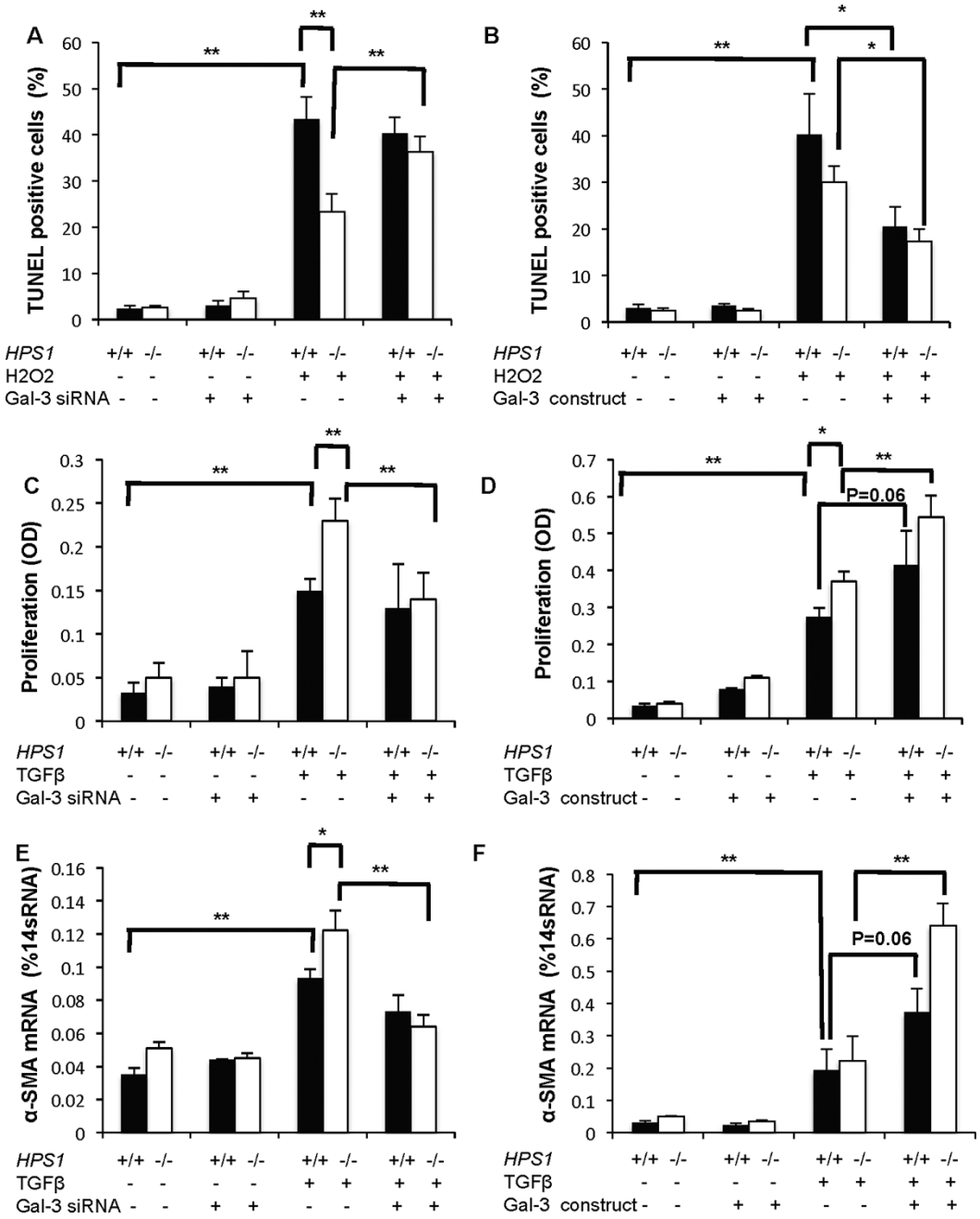

Figure 5. Effects of intracellular Gal-3 on fibroblasts from *pale ear* mice

Primary lung fibroblasts were extracted from WT and *pale ear* mice. In (A) and (B), cells were pre-treated with Gal-3 siRNA or Gal-3 overexpression construct, and H2O2 was used to induce cell death. TUNEL staining was performed and TUNEL-positive cells were counted. In (C) and (D), cells were pre-treated with Gal-3 siRNA or Gal-3 overexpression construct, and TGF-β was used to induce cell proliferation. Cell proliferation was determined by WST-1 assay. In (E) and (F), cells were pre-treated with Gal-3 siRNA or Gal-3 overexpression construct, and TGF-β was used to induce cell differentiation. Alpha-SMA expression was measured to quantitate myofibroblast differentiation. Each experiment

was undertaken at least 3 times. The noted values represent the mean ± SEM of a minimum of 3 separate experiments. *$p \leq 0.05$,**$p \leq 0.01$.

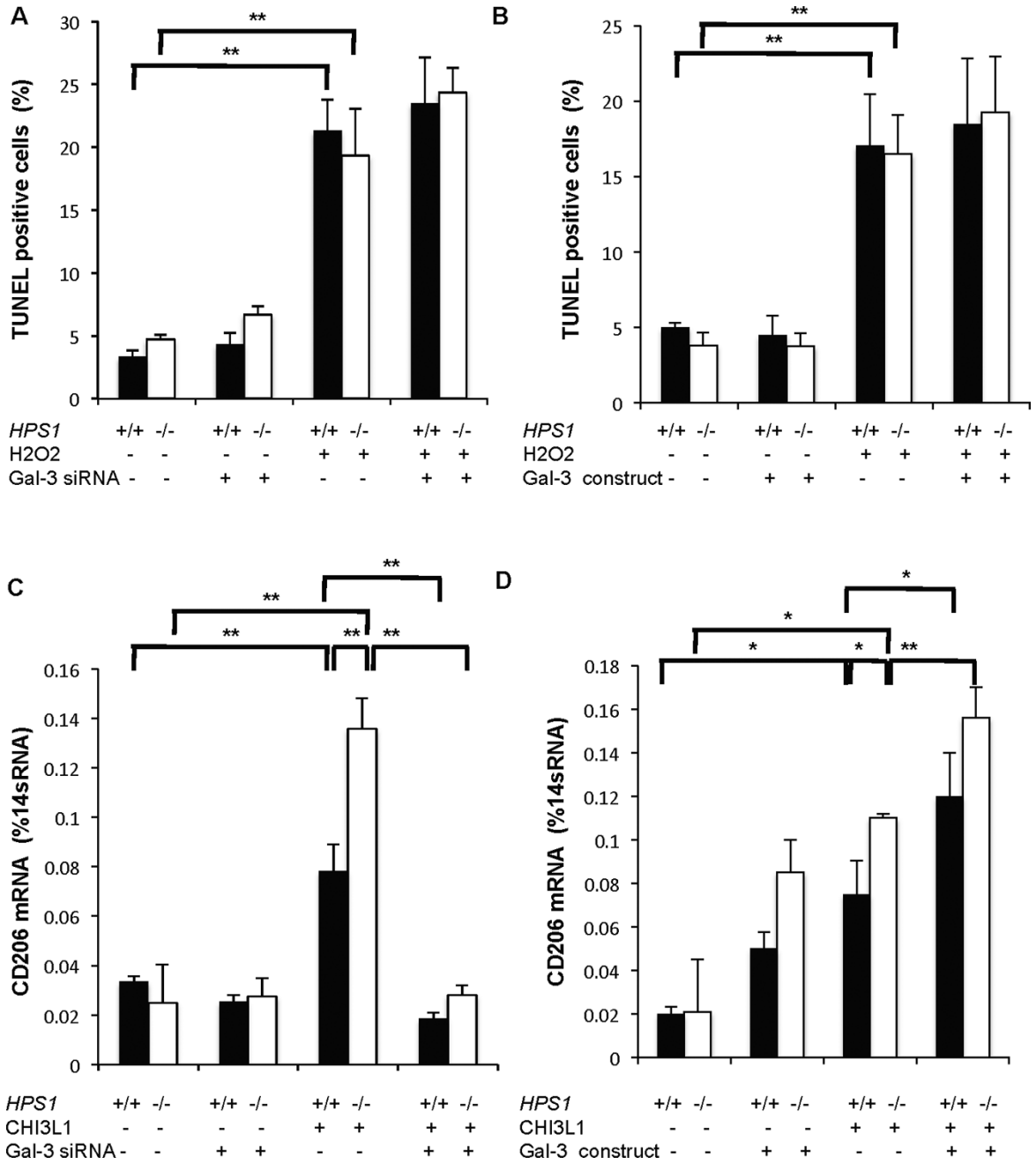

Figure 6. Effects of intracellular Gal-3 on macrophages from *pale ear* mice

Primary alveolar macrophages were obtained from WT and *pale ear* mice. In (A) and (B), cells were pretreated with Gal-3 siRNA, a Gal-3 overexpression construct or appropriate controls and H_2O_2 was used to induce cell death. TUNEL staining was performed and TUNEL-positive cells were counted. In (C) and (D), cells were pretreated with Gal-3 siRNA, a Gal-3 overexpression construct or appropriate controls and CHI3L1 was used to induce M2 macrophage differentiation. CD206 expression was measured as an index of M2 differentiation. Each experiment was undertaken at least 3 times. The noted values represent the mean ± SEM of a minimum of 3 experiments. *$p \leq 0.05$,**$p \leq 0.01$.

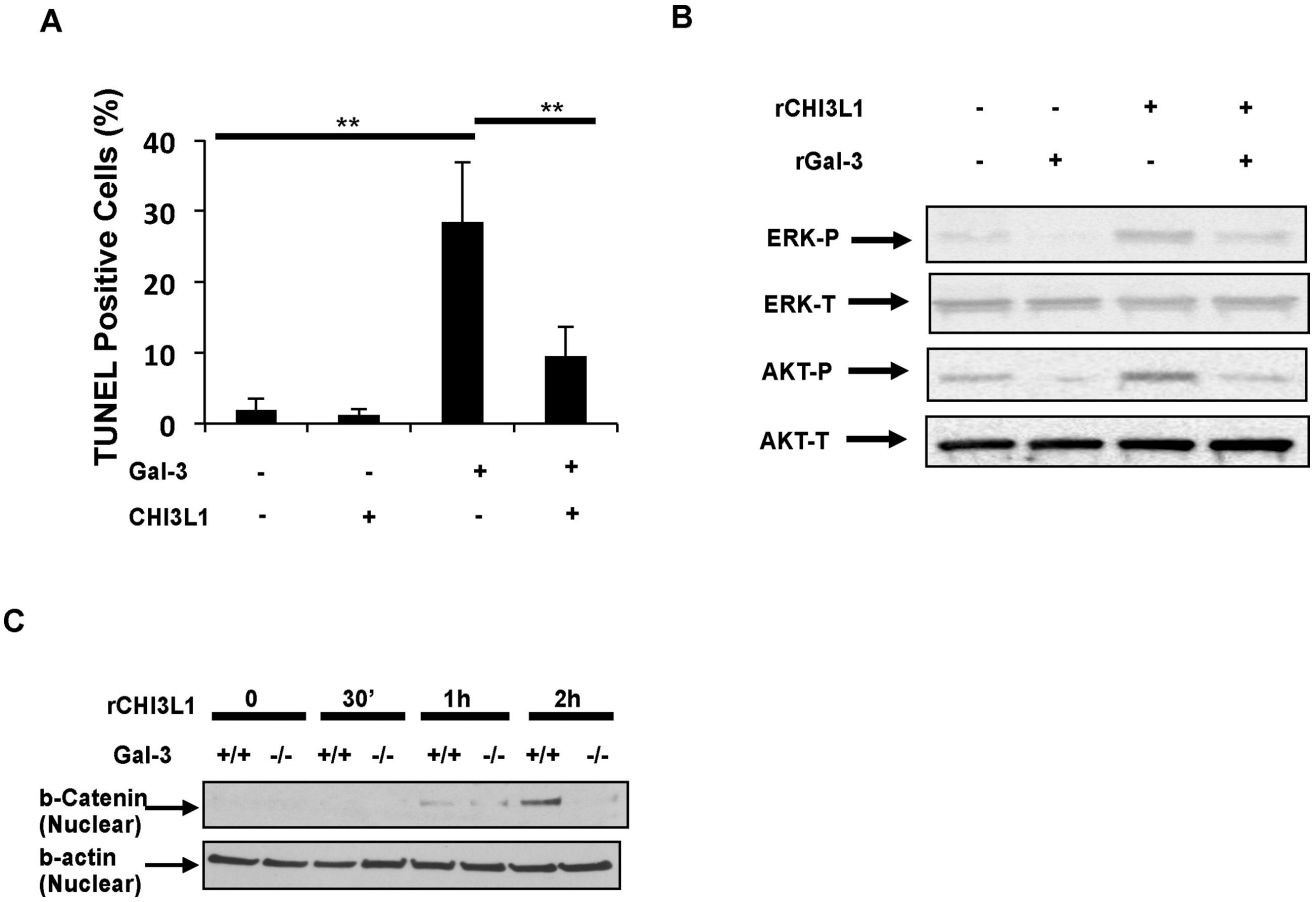

Figure 7. Gal-3 regulation of CHI3L1-induced antiapoptotic and Wnt/b-catenin signaling

(A) MLE 12 cells were incubated with rGal-3, rCHI3L1 or appropriate controls for 24 hours and cellular apoptosis was evaluated by TUNEL staining. (B) MLE 12 cells were incubated with rGal-3 or appropriate controls in the presence or absence of rCHI3L1and ERK and AKT activation were assessed by Western blot. (C) Peritoneal macrophages from wild type or Gal-$3^{-/-}$ mice were incubated for up to 2 hours for with rCHI3L1 (500 ng/ml), and nuclear β-catenin was assessed. Each experiment was undertaken at least 3 times. The values in panel A represent the mean ± SEM of a minimum of 3 experiments. **$p \leq 0.01$. Panels B and C are representative of a minimum of 3 separate experiments.

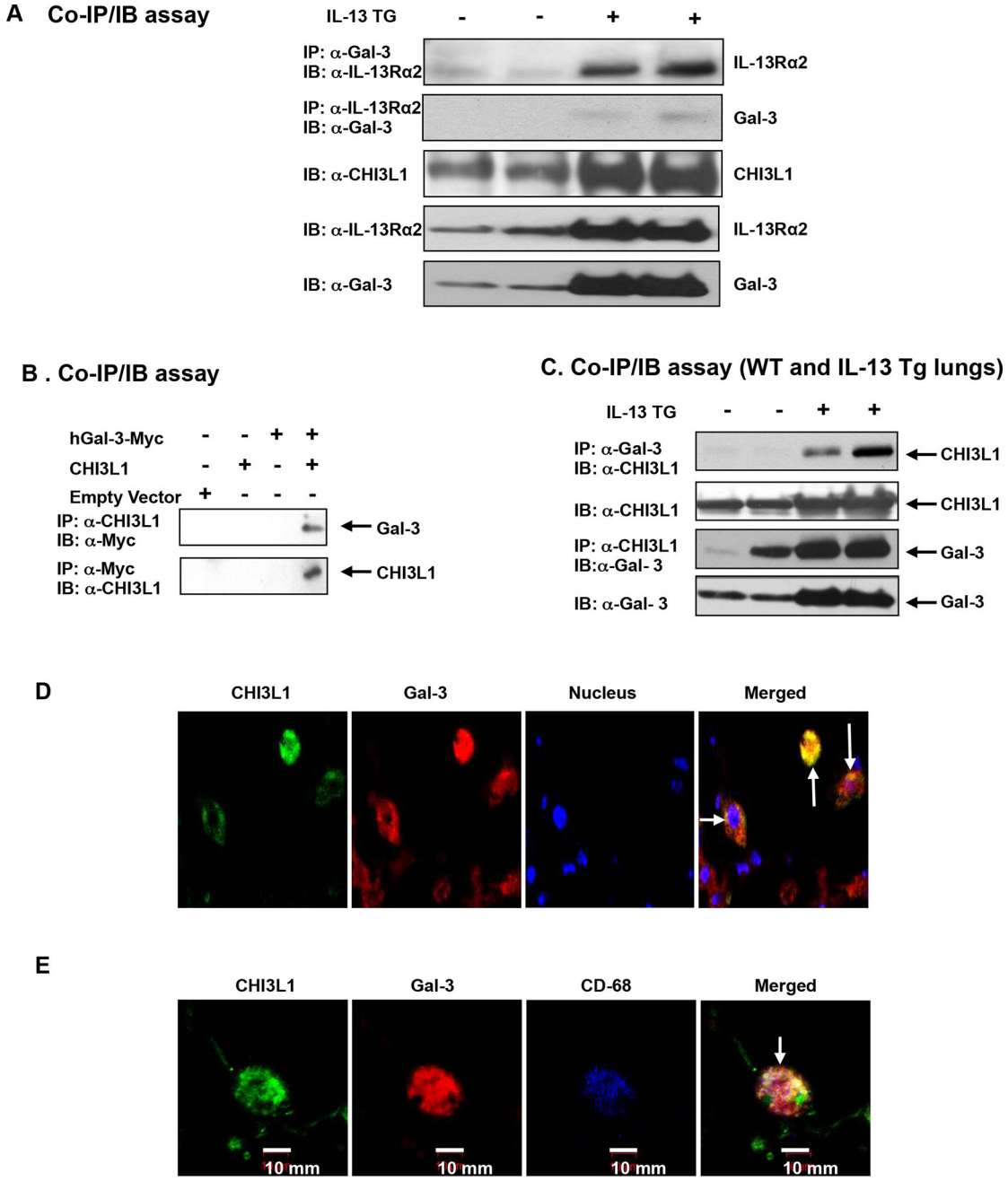

Figure 8. Gal-3 binds to IL-13Rα2 and CHI3L1

(A) Gal-3 binds to IL-13Rα2 *in vivo*. Lung lysates were prepared from WT and IL-13 transgenic mice and immunoprecipitated (IP) with anti-Gal--3 or anti-IL-13Rα2 and the precipitates were evaluated using immunoblot (IB) analysis as noted. (B) Gal-3 binds to CHI3L1 *in vitro*. A549 cells were transfected with CHI3L1 (hCHI3L1) and/or human Gal-3-myc tag (hGal-3-Myc). Cell lysates were then prepared, immunoprecipitated (IP) with either anti-CHI3L1 or anti-Myc, and the precipitates were evaluated using immunoblot (IB) analysis as noted. (C) Gal-3 binds to CHI3L1 *in vivo*. Lung lysates were prepared from WT and IL-13 transgenic mice. They were then immunoprecipitated (IP) with anti-CHI3L1 or

anti-Gal-3 and the precipitates were evaluated using immunoblot (IB) analysis as noted. (D) Gal-3 co-localizes with CHI3L1. Double-label IHC was used to localize CHI3L1 and Gal-3 in lungs from IL-13 Tg mice using antibodies to CHI3L1 and Gal-3. (E) Gal-3 co-localizes with CHI3L1 in macrophages. Triple-label IHC to localize of CHI3L1 and Gal-3 in the macrophages in lungs from IL-13 Tg mice using antibodies to CHI3L1, Gal-3, and cell-specific markers of macrophages (anti-CD68). The arrows highlight cells with colocalized moieties. Each experiment was undertaken at least 3 times. Panels A-C are representative of a minimum of 3 separate experiments. Images in D and E are representative of 3 mice.

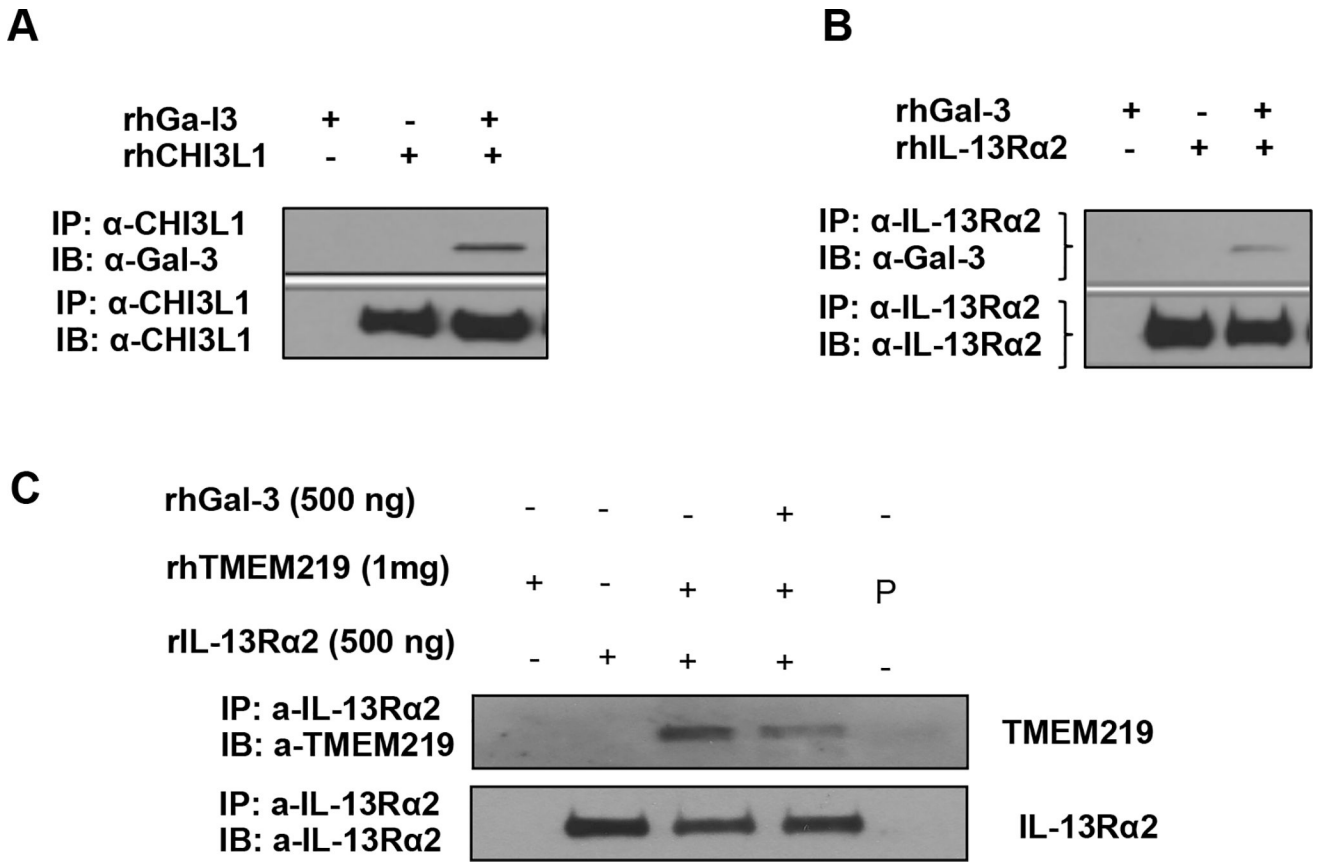

Figure 9. Gal-3 competes with TMEM219 for IL-13Rα2

In these experiments recombinant proteins (rhGal-3, rhIL-13Rα2 and rhTMEM219) were employed. Co-immunoprecipitation (Co-IP) and immunoblot (IB) evaluations demonstrated that Gal-3 binds with (A) CHI3L1 and (B) IL-13Rα2. (C) In these experiments, we combined rhTMEM219 and rhIL-13Rα2 in presence or absence of rhGal-3. Immunoprecipitation (IP) was then undertaken with anti-IL-13Rα2 and the precipitates were evaluated using immunoblot (IB) analysis as noted. Each experiment was undertaken at least 3 times. Panels A-C are representative of a minimum of 3 separate experiments.